axioms

MDPI

Article

Combined Compact Symplectic Schemes for the Solution of Good Boussinesq Equations

Zhenyu Lang [1], Xiuling Yin [2,*], Yanqin Liu [2], Zhiguo Chen [2] and Shuxia Kong [2]

[1] School of Mathematics and Statistics, Shandong University of Technology, Zibo 255049, China; 23411011065@sdut.edu.cn
[2] School of Mathematics and Big Data, Dezhou University, Dezhou 253023, China; chenzhiguo@dzu.edu.cn (Z.C.); kongshuxia@dzu.edu.cn (S.K.)
* Correspondence: yinllmm@163.com; Tel.: +86-1831-591-6282

Abstract: Good Boussinesq equations are considered in this work. First, we apply three combined compact schemes to approximate spatial derivatives of good Boussinesq equations. Then, three fully discrete schemes are developed based on a symplectic scheme in the time direction, which preserves the symplectic structure. Meanwhile, the convergence and conservation of the fully discrete schemes are analyzed. Finally, we present numerical experiments to confirm our theoretical analysis. Both our analysis and numerical tests indicate that the fully discrete schemes are efficient in solving the spatial derivative mixed equation.

Keywords: Hamiltonian system; good Boussinesq equation; symplectic scheme; combined compact scheme; conservation

MSC: 65M06; 65M12; 65Z05; 70H15

check for updates

Citation: Lang, Z.; Yin, X.; Liu, Y.; Chen, Z.; Kong, S. Combined Compact Symplectic Schemes for the Solution of Good Boussinesq Equations. *Axioms* **2024**, *13*, 574. https://doi.org/10.3390/axioms13090574

Academic Editors: Branislav Randjelovic and Branislav Vlahovic

Received: 19 June 2024
Revised: 3 August 2024
Accepted: 11 August 2024
Published: 23 August 2024

Copyright: © 2024 by the authors. Licensee MDPI, Basel, Switzerland. This article is an open access article distributed under the terms and conditions of the Creative Commons Attribution (CC BY) license (https://creativecommons.org/licenses/by/4.0/).

1. Introduction

Boussinesq equations are important mathematical–physical models for characterizing ocean mixing, atmospheric convection, and intra-Earth convection. They play a key role in fields such as Earth sciences, meteorology, and oceanography. The study of Boussinesq equations is of great value because it helps us to better understand hydrodynamic behavior, especially in terms of thermal convection, ocean currents, and atmospheric phenomena. In addition, the study of Boussinesq equations is essential for the development of numerical models for weather forecasting, climate research, and oceanography. Such studies have also helped to uncover the fundamental principles that govern fluid motion and heat transfer, contributing to advances in fields such as engineering, environmental science, and geophysics. The good Boussinesq (GB) equation and its various extensions have been broadly analyzed in the existing literature, such as a closed-form solution for the two-soliton interaction in [1], a highly complicated mechanism for the solitary wave interaction in [2], and the nonlinear stability and convergence of some simple finite difference schemes in [3]. Among recent works concerning the numerical solution of PDEs, a significant number address the Schrödinger equation; see [4–11]. In [5,6], the authors use the Cubic B-Spline Galerkin Method. This method has also been studied for the MRLW equation in [12]. In [11], the authors use a combined compact difference method to solve the Schrödinger equation, and this scheme preserves the structure. This method originated from [13], and it can also be found in [14–17]. In addition, many works related to GB equations can be found in [18–24]. Boussinesq equations have also been investigated in [25,26].

In solving PDEs numerically, high-order compact (HOC) schemes are often used to discretize spatial derivatives. For example, HOC schemes have been applied to solve steady convection–diffusion equations [15], nonlinear Schrödinger equations [11], Klein–Gordon–Schrödinger equations [27], and GB equations [20]. Compared with general finite difference schemes, HOC

schemes have the advantages of smaller error rates and higher accuracy under the same calculation amount. However, for PDEs with multiple-order spatial derivatives, such as the good Boussinesq equation $u_{tt} = -u_{xxxx} + u_{xx} + \left(u^2\right)_{xx}$, the advantages of classical HOC schemes are often offset. If multiple HOC schemes are used to discretize multiple spatial derivatives simultaneously, it is necessary to perform multiple matrix inverse operations, which will reduce the computational efficiency and affect the accuracy. In [11], the combined high-order compact (CHOC) scheme is used to approximate PDEs with multiple-order spatial derivatives and achieve some discrete conservation laws, and the proposed CHOC scheme overcomes the above shortcomings of the compact scheme and is worth popularizing. In this work, we study the CHOC schemes of GB equations with two spatial derivatives.

In this work, three CHOC schemes for good Boussinesq equations are derived. Applying a Taylor analysis to an equality combining the solution u and its first derivative and second derivative yields the first three-point CHOC scheme. This scheme has sixth-order precision and extensive applications. Then, similarly, we propose the second three-point eight-order scheme by using a combination of the first, second, and third derivatives of the solution. Since the two schemes have a large number of matrix operations and complex formulations, the third scheme is designed finally by combining the solution and its second derivative and fourth derivative, which greatly simplifies the matrix operations and ensures certain accuracy. In this scheme, through simpler computation, the relationship between the solution and its fourth-order derivative, as well as the relationship between the solution and its second-order derivative, can be directly obtained, which cannot be achieved with the first two schemes described in this work. Finally, we use the three schemes to simulate a motion invariant and a conservation law and summarize the structure-preserving property of these schemes. At the same time, compared with a three-point compact scheme with sixth-order accuracy derived by Chu and Fan in 1998 [13], our schemes are more accurate for GB equations.

In this work, we consider fully discrete schemes for the linear good Boussinesq equation

$$\partial_t^2 u = \partial_x^2 u - \partial_x^4 u, \tag{1}$$

where $0 \le x \le L, t > 0$, L is a constant. The following nonlinear good Boussinesq equation is also numerically solved, as follows:

$$\partial_t^2 u = \partial_x^2 u - \partial_x^4 u + \partial_x^2 (u^2). \tag{2}$$

We consider the initial conditions and periodic boundary conditions as follows:

$$u(t,0) = u(t,L),\ u(0,x) = f_1(x), u_t(0,x) = f_2(x), 0 \le x \le L. \tag{3}$$

2. Establishment of the CHOC Scheme

In this work, we introduce three schemes for the discretization of spatial derivatives. To detail the CHOC scheme, we introduce a uniform grid $x_0 < x_1 \cdots < x_N$ with $x_j = x_0 + jh$ and $h = \frac{x_L - x_0}{N}, j = 1, 2, \cdots, N$. First, we introduce the first scheme (4) and (5)

$$\alpha_1\left(u_{j+1}^{'} + u_{j-1}^{'}\right) + u_j^{'} + \beta_1 h\left(u_{j+1}^{''} - u_{j-1}^{''}\right) + \gamma_1 \frac{u_{j+1} - u_{j-1}}{h} = 0, \tag{4}$$

$$\alpha_2\left(\frac{u_{j+1}^{'} - u_{j-1}^{'}}{h}\right) + u_j^{''} + \beta_2\left(u_{j+1}^{''} + u_{j-1}^{''}\right) + \gamma_2 \frac{u_{j+1} - 2u_j + u_{j-1}}{h^2} = 0, \tag{5}$$

where $\alpha_1, \beta_1, \gamma_1$ and $\alpha_2, \beta_2, \gamma_2$ are coefficients to be determined according to the accuracy of the approximation. The three-point CHOC scheme for the combination of the first and second derivatives aims to relate $u_j, u_j^{'}, u_j^{''}$ to their neighbors $u_{j-1}, u_{j-1}^{'}, u_{j-1}^{''}$ and $u_{j+1}, u_{j+1}^{'}, u_{j+1}^{''}$.

This scheme approximates the first-order derivative and second-order derivative of u separately using the above combinations to numerically solve the Schrödinger equation in [11].

By applying Taylor expansion to Equations (4) and (5), we can obtain the following Tables 1 and 2. Here, the last row denotes the summation of each corresponding column. The tables related to Taylor expansion and discussed subsequently are similarly constructed.

Table 1. Taylor series of scheme (4).

Term	$u_j h^{-1}$	$u_j^{'}$	$u_j^{''} h$	$u_j^{'''} h^2$	$u_j^{(4)} h^3$	$u_j^{(5)} h^4$	$u_j^{(6)} h^5$	$u_j^{(7)} h^6$	$u_j^{(8)} h^7$
$\alpha_1 u_{j+1}^{'}$	0	α_1	α_1	$\frac{\alpha_1}{2!}$	$\frac{\alpha_1}{3!}$	$\frac{\alpha_1}{4!}$	$\frac{\alpha_1}{5!}$	$\frac{\alpha_1}{6!}$	$\frac{\alpha_1}{7!}$
$\alpha_1 u_{j-1}^{'}$	0	α_1	$-\alpha_1$	$\frac{\alpha_1}{2!}$	$-\frac{\alpha_1}{3!}$	$\frac{\alpha_1}{4!}$	$-\frac{\alpha_1}{5!}$	$\frac{\alpha_1}{6!}$	$-\frac{\alpha_1}{7!}$
$u_j^{'}$	0	1	0	0	0	0	0	0	0
$\beta_1 u_{j+1}^{''} h$	0	0	β_1	β_1	$\frac{\beta_1}{2!}$	$\frac{\beta_1}{3!}$	$\frac{\beta_1}{4!}$	$\frac{\beta_1}{5!}$	$\frac{\beta_1}{6!}$
$-\beta_1 u_{j-1}^{''} h$	0	0	$-\beta_1$	β_1	$-\frac{\beta_1}{2!}$	$\frac{\beta_1}{3!}$	$-\frac{\beta_1}{4!}$	$\frac{\beta_1}{5!}$	$-\frac{\beta_1}{6!}$
$\frac{\gamma_1}{h} u_{j+1}$	γ_1	γ_1	$\frac{\gamma_1}{2!}$	$\frac{\gamma_1}{3!}$	$\frac{\gamma_1}{4!}$	$\frac{\gamma_1}{5!}$	$\frac{\gamma_1}{6!}$	$\frac{\gamma_1}{7!}$	$\frac{\gamma_1}{8!}$
$-\frac{\gamma_1}{h} u_{j-1}$	$-\gamma_1$	γ_1	$-\frac{\gamma_1}{2!}$	$\frac{\gamma_1}{3!}$	$-\frac{\gamma_1}{4!}$	$\frac{\gamma_1}{5!}$	$-\frac{\gamma_1}{6!}$	$\frac{\gamma_1}{7!}$	$-\frac{\gamma_1}{8!}$
Σ	0	y_{11}	0	y_{12}	0	y_{13}	0	y_{14}	0

Table 2. Taylor series of scheme (5).

Term	$u_j h^{-2}$	$u_j^{'} h^{-1}$	$u_j^{''}$	$u_j^{'''} h$	$u_j^{(4)} h^2$	$u_j^{(5)} h^3$	$u_j^{(6)} h^4$	$u_j^{(7)} h^5$	$u_j^{(8)} h^6$
$\frac{\alpha_2}{h} u_{j+1}^{'}$	0	α_2	α_2	$\frac{\alpha_2}{2!}$	$\frac{\alpha_2}{3!}$	$\frac{\alpha_2}{4!}$	$\frac{\alpha_2}{5!}$	$\frac{\alpha_2}{6!}$	$\frac{\alpha_2}{7!}$
$-\frac{\alpha_2}{h} u_{j-1}^{'}$	0	$-\alpha_2$	α_2	$-\frac{\alpha_2}{2!}$	$\frac{\alpha_2}{3!}$	$-\frac{\alpha_2}{4!}$	$\frac{\alpha_2}{5!}$	$-\frac{\alpha_2}{6!}$	$\frac{\alpha_1}{7!}$
$u_j^{''}$	0	0	1	0	0	0	0	0	0
$\beta_2 u_{j+1}^{''}$	0	0	β_2	β_2	$\frac{\beta_2}{2!}$	$\frac{\beta_2}{3!}$	$\frac{\beta_2}{4!}$	$\frac{\beta_2}{5!}$	$\frac{\beta_2}{6!}$
$\beta_2 u_{j-1}^{''}$	0	0	β_2	$-\beta_2$	$\frac{\beta_2}{2!}$	$-\frac{\beta_2}{3!}$	$\frac{\beta_2}{4!}$	$-\frac{\beta_2}{5!}$	$\frac{\beta_2}{6!}$
$\frac{\gamma_2}{h^2} u_{j+1}$	γ_2	γ_2	$\frac{\gamma_2}{2!}$	$\frac{\gamma_2}{3!}$	$\frac{\gamma_2}{4!}$	$\frac{\gamma_2}{5!}$	$\frac{\gamma_2}{6!}$	$\frac{\gamma_2}{7!}$	$\frac{\gamma_2}{8!}$
$-2\frac{\gamma_2}{h^2} u_j$	$-2\gamma_2$	0	0	0	0	0	0	0	0
$\frac{\gamma_2}{h^2} u_{j-1}$	γ_2	$-\gamma_2$	$\frac{\gamma_2}{2!}$	$-\frac{\gamma_2}{3!}$	$\frac{\gamma_2}{4!}$	$-\frac{\gamma_2}{5!}$	$\frac{\gamma_2}{6!}$	$-\frac{\gamma_2}{7!}$	$\frac{\gamma_2}{8!}$
Σ	0	0	y_{21}	0	y_{22}	0	y_{23}	0	y_{24}

To obtain this scheme with sixth-order convergence, the above coefficients must satisfy the following algebraic equations:

$$\begin{cases} y_{11} = 2(\alpha_1 + \gamma_1) + 1 = 0, \\ y_{12} = \alpha_1 + 2\left(\beta_1 + \frac{\gamma_1}{3!}\right) = 0, \\ y_{13} = 2\left(\frac{\alpha_1}{4!} + \frac{\beta_1}{3!} + \frac{\gamma_1}{5!}\right) = 0, \end{cases} \tag{6}$$

and

$$\begin{cases} y_{21} = 2(\alpha_2 + \beta_2) + \gamma_2 + 1 = 0, \\ y_{22} = \frac{\alpha_2}{3} + \beta_2 + \frac{\gamma_2}{12} = 0, \\ y_{23} = \frac{\alpha_2}{5!} + \frac{\beta_2}{4!} + \frac{\gamma_2}{6!} = 0. \end{cases} \tag{7}$$

The solutions of the above equations are

$$\alpha_1 = \frac{7}{16}, \beta_1 = -\frac{1}{16}, \gamma_1 = -\frac{15}{16},$$

and

$$\alpha_2 = \frac{9}{8}, \beta_2 = -\frac{1}{8}, \gamma_2 = -3.$$

Therefore, schemes (4) and (5) possess the specific forms

$$\frac{1}{16}\left(7u'_{j+1} + 16u'_j + 7u'_{j-1}\right) - \frac{h}{16}\left(u''_{j+1} - u''_{j-1}\right) = \frac{15}{16h}(u_{j+1} - u_{j-1}), \tag{8}$$

$$\frac{9}{8h}\left(u'_{j+1} - u'_{j-1}\right) - \frac{1}{8}\left(u''_{j+1} - 8u''_j + u''_{j-1}\right) = \frac{3}{h^2}(u_{j+1} - 2u_j + u_{j-1}). \tag{9}$$

After conducting a thorough analysis, it is determined that this scheme has relatively limited applicability. Its usage often necessitates complex matrix operations, and it is insufficient for differential equations involving certain high-order derivatives. In the good Boussinesq equation under study in this work, a fourth-order spatial derivative is involved. To obtain the numerical solutions of good Boussinesq equations, we require the discretization of $\partial_x^4 u$ and $\partial_x^2 u$. Here, we adopt the combination of the function values of u and its first-order derivative and second-order derivative to represent the fourth-order spatial derivative

$$u_j^{(4)} = -\frac{36}{h^4}(u_{j+1} - 2u_j + u_{j-1}) + \frac{21}{h^3}\left(u'_{j+1} + u'_{j-1}\right) - \frac{3}{h^2}\left(u''_{j+1} + u''_{j-1}\right). \tag{10}$$

Under periodic boundary conditions, by combining (8) and (9), we have

$$\begin{cases} \mathrm{A}_{11}U_x + \mathrm{A}_{12}U_{xx} = \mathrm{A}_{13}U, \\ \mathrm{A}_{21}U_x + \mathrm{A}_{22}U_{xx} = \mathrm{A}_{23}U. \end{cases} \tag{11}$$

where

$$\mathrm{A}_{11} = \frac{1}{16}\begin{bmatrix} 16 & 7 & & & 7 \\ 7 & 16 & 7 & & \\ & \ddots & \ddots & \ddots & \\ & & 7 & 16 & 7 \\ 7 & & & 7 & 16 \end{bmatrix}, \mathrm{A}_{12} = -\frac{\mathrm{h}}{16}\begin{bmatrix} 0 & 1 & & & -1 \\ -1 & 0 & 1 & & \\ & \ddots & \ddots & \ddots & \\ & & -1 & 0 & 1 \\ 1 & & & -1 & 0 \end{bmatrix}, \mathrm{A}_{13} = \frac{15}{16\mathrm{h}}\begin{bmatrix} 0 & 1 & & & -1 \\ -1 & 0 & 1 & & \\ & \ddots & \ddots & \ddots & \\ & & -1 & 0 & 1 \\ 1 & & & -1 & 0 \end{bmatrix},$$

$$\mathrm{A}_{21} = \frac{9}{8\mathrm{h}}\begin{bmatrix} 0 & 1 & & & -1 \\ -1 & 0 & 1 & & \\ & \ddots & \ddots & \ddots & \\ & & -1 & 0 & 1 \\ 1 & & & -1 & 0 \end{bmatrix}, \mathrm{A}_{22} = -\frac{1}{8}\begin{bmatrix} -8 & 1 & & & 1 \\ 1 & -8 & 1 & & \\ & \ddots & \ddots & \ddots & \\ & & 1 & -8 & 1 \\ 1 & & & 1 & -8 \end{bmatrix}, \mathrm{A}_{23} = \frac{3}{\mathrm{h}^2}\begin{bmatrix} -2 & 1 & & & 1 \\ 1 & -2 & 1 & & \\ & \ddots & \ddots & \ddots & \\ & & 1 & -2 & 1 \\ 1 & & & 1 & -2 \end{bmatrix}.$$

By solving (11), we can obtain $U_x = \mathrm{G} \cdot U, U_{xx} = \mathrm{H} \cdot U, \mathrm{G} = \mathrm{A}^{-1}\mathrm{B}, \mathrm{H} = \mathrm{A}^{-1}\mathrm{C}$, where $\mathrm{A} = \mathrm{A}_{11}\mathrm{A}_{22} - \mathrm{A}_{12}\mathrm{A}_{21}, \mathrm{B} = \mathrm{A}_{22}\mathrm{A}_{13} - \mathrm{A}_{12}\mathrm{A}_{23}, \mathrm{C} = \mathrm{A}_{11}\mathrm{A}_{23} - \mathrm{A}_{21}\mathrm{A}_{13}$. For (10), we have

$$\begin{bmatrix} \mathrm{u}_1^{(4)} \\ \mathrm{u}_2^{(4)} \\ \vdots \\ \mathrm{u}_{N-1}^{(4)} \\ \mathrm{u}_N^{(4)} \end{bmatrix} = -\frac{36}{\mathrm{h}^4}\begin{bmatrix} -2 & 1 & & & 1 \\ 1 & -2 & 1 & & \\ & \ddots & \ddots & \ddots & \\ & & 1 & -2 & 1 \\ 1 & & & 1 & -2 \end{bmatrix}\begin{bmatrix} \mathrm{u}_1 \\ \mathrm{u}_2 \\ \vdots \\ \mathrm{u}_{N-1} \\ \mathrm{u}_N \end{bmatrix} + \frac{21}{\mathrm{h}^3}\begin{bmatrix} 0 & 1 & & & -1 \\ -1 & 0 & 1 & & \\ & \ddots & \ddots & \ddots & \\ & & -1 & 0 & 1 \\ 1 & & & -1 & 0 \end{bmatrix}\begin{bmatrix} \mathrm{u}'_1 \\ \mathrm{u}'_2 \\ \vdots \\ \mathrm{u}'_{N-1} \\ \mathrm{u}'_N \end{bmatrix} - \frac{3}{\mathrm{h}^2}\begin{bmatrix} 0 & 1 & & & 1 \\ 1 & 0 & 1 & & \\ & \ddots & \ddots & \ddots & \\ & & 1 & 0 & 1 \\ 1 & & & 1 & 0 \end{bmatrix}\begin{bmatrix} \mathrm{u}''_1 \\ \mathrm{u}''_2 \\ \vdots \\ \mathrm{u}''_{N-1} \\ \mathrm{u}''_N \end{bmatrix},$$

where

$$B_1 = -\frac{3}{h^2}\begin{bmatrix} 0 & 1 & & & 1 \\ 1 & 0 & 1 & & \\ & \ddots & \ddots & \ddots & \\ & & 1 & 0 & 1 \\ 1 & & & 1 & 0 \end{bmatrix}.$$

By substituting $U_x = G \cdot U, U_{xx} = H \cdot U$ into this, the above expression can be represented as follows:

$$\partial_x^4 U = -\frac{12}{\mathrm{h}^2}\mathrm{A}_{23} \cdot U + \frac{56}{3h^2}\mathrm{A}_{21}\mathrm{G} \cdot U + \mathrm{B}_1\mathrm{H} \cdot U. \tag{12}$$

Let $\mathrm{M} = \mathrm{B}_1 \cdot \mathrm{H} + \frac{56}{3\mathrm{h}^2}\mathrm{A}_{21} \cdot \mathrm{G} - \frac{12}{\mathrm{h}^2}\mathrm{A}_{23}$. We will use the following schemes for the spatial derivatives:

$$\begin{cases} \partial_x^4 U = \mathrm{M} \cdot U, \\ \partial_x^2 U = \mathrm{H} \cdot U. \end{cases} \tag{13}$$

Next, we will obtain the second CHOC scheme with eighth-order accuracy with the combination of the first, second, and third derivatives relating $u_j, u_j^{'}, u_j^{''}, u_j^{'''}$ to their neighbors $u_{\mathrm{j}-1}, u_{j-1}^{'}, u_{j-1}^{''}, u_{j-1}^{'''}$ and $u_{j+1}, u_{j+1}^{'}, u_{j+1}^{''}, u_{j+1}^{'''}$. The generalization of (4) and (5) to the case of three derivatives similarly yields the following CHOC scheme:

$$\alpha_1\left(u_{j+1}^{'} + u_{j-1}^{'}\right) + u_j^{'} + \beta_1 h\left(u_{j+1}^{''} - u_{j-1}^{''}\right) + \omega_1 h^2\left(u_{j+1}^{'''} + u_{j-1}^{'''}\right) + \gamma_1\frac{u_{j+1} - u_{j-1}}{h} = 0, \tag{14}$$

$$\alpha_2\left(\frac{u_{j+1}^{'} - u_{j-1}^{'}}{h}\right) + u_j^{''} + \beta_2\left(u_{j+1}^{''} + u_{j-1}^{''}\right) + \omega_2 h\left(u_{j+1}^{'''} - u_{j-1}^{'''}\right) + \gamma_2\frac{u_{j+1} - 2u_j + u_{j-1}}{h^2} = 0, \tag{15}$$

$$\alpha_3\left(\frac{u_{j+1}^{'} + u_{j-1}^{'}}{h}\right) + u_j^{'''} + \beta_3\left(\frac{u_{j+1}^{''} - u_{j-1}^{''}}{h}\right) + \omega_3\left(u_{j+1}^{'''} + u_{j-1}^{'''}\right) + \gamma_3\frac{u_{j+1} - u_{j-1}}{h^3} = 0, \tag{16}$$

where $\alpha_1, \beta_1, \omega_1, \gamma_1$ and $\alpha_2, \beta_2, \omega_2, \gamma_2$ and $\alpha_3, \beta_3, \omega_3, \gamma_3$ are coefficients to be determined according to the accuracy of the approximation. Through the Taylor expansion of Equations (14)–(16), we can obtain Tables 3–5.

Table 3. Taylor series of scheme (14).

Term	$u_j h^{-1}$	$u_j^{'}$	$u_j^{''}h$	$u_j^{'''}h^2$	$u_j^{(4)}h^3$	$u_j^{(5)}h^4$	$u_j^{(6)}h^5$	$u_j^{(7)}h^6$	$u_j^{(8)}h^7$
$\alpha_1 u_{j+1}^{'}$	0	α_1	α_1	$\frac{\alpha_1}{2!}$	$\frac{\alpha_1}{3!}$	$\frac{\alpha_1}{4!}$	$\frac{\alpha_1}{5!}$	$\frac{\alpha_1}{6!}$	$\frac{\alpha_1}{7!}$
$\alpha_1 u_{j-1}^{'}$	0	α_1	$-\alpha_1$	$\frac{\alpha_1}{2!}$	$-\frac{\alpha_1}{3!}$	$\frac{\alpha_1}{4!}$	$-\frac{\alpha_1}{5!}$	$\frac{\alpha_1}{6!}$	$-\frac{\alpha_1}{7!}$
$u_j^{'}$	0	1	0	0	0	0	0	0	0
$\beta_1 u_{j+1}^{''}h$	0	0	β_1	β_1	$\frac{\beta_1}{2!}$	$\frac{\beta_1}{3!}$	$\frac{\beta_1}{4!}$	$\frac{\beta_1}{5!}$	$\frac{\beta_1}{6!}$
$-\beta_1 u_{j-1}^{''}h$	0	0	$-\beta_1$	β_1	$-\frac{\beta_1}{2!}$	$\frac{\beta_1}{3!}$	$-\frac{\beta_1}{4!}$	$\frac{\beta_1}{5!}$	$-\frac{\beta_1}{6!}$
$\omega_1 u_{j+1}^{'''}h^2$	0	0	0	ω_1	ω_1	$\frac{\omega_1}{2!}$	$\frac{\omega_1}{3!}$	$\frac{\omega_1}{4!}$	$\frac{\omega_1}{5!}$
$\omega_1 u_{j-1}^{'''}h^2$	0	0	0	ω_1	$-\omega_1$	$\frac{\omega_1}{2!}$	$-\frac{\omega_1}{3!}$	$\frac{\omega_1}{4!}$	$-\frac{\omega_1}{5!}$
$\frac{\gamma_1}{h}u_{j+1}$	γ_1	γ_1	$\frac{\gamma_1}{2!}$	$\frac{\gamma_1}{3!}$	$\frac{\gamma_1}{4!}$	$\frac{\gamma_1}{5!}$	$\frac{\gamma_1}{6!}$	$\frac{\gamma_1}{7!}$	$\frac{\gamma_1}{8!}$
$-\frac{\gamma_1}{h}u_{j-1}$	$-\gamma_1$	γ_1	$-\frac{\gamma_1}{2!}$	$\frac{\gamma_1}{3!}$	$-\frac{\gamma_1}{4!}$	$\frac{\gamma_1}{5!}$	$-\frac{\gamma_1}{6!}$	$\frac{\gamma_1}{7!}$	$-\frac{\gamma_1}{8!}$
Σ	0	y_{11}	0	y_{12}	0	y_{13}	0	y_{14}	0

To obtain these schemes with the eighth order, they must satisfy the algebraic equations

$$\begin{cases} y_{11} = 2(\alpha_1 + \gamma_1) + 1 = 0, \\ y_{12} = \alpha_1 + 2\left(\beta_1 + \omega_1 + \frac{\gamma_1}{3!}\right) = 0, \\ y_{13} = 2\left(\frac{\alpha_1}{4!} + \frac{\beta_1}{3!} + \frac{\omega_1}{2!} + \frac{\gamma_1}{5!}\right) = 0, \\ y_{14} = 2\left(\frac{\alpha_1}{6!} + \frac{\beta_1}{5!} + \frac{\omega_1}{4!} + \frac{\gamma_1}{7!}\right) = 0, \end{cases} \tag{17}$$

and

$$\begin{cases} y_{21} = 2\left(\alpha_2 + \beta_2 + \frac{\gamma_2}{2!}\right) + 1 = 0, \\ y_{22} = 2\left(\frac{\alpha_2}{3!} + \frac{\beta_2}{2!} + \omega_2 + \frac{\gamma_2}{4!}\right) = 0, \\ y_{23} = 2\left(\frac{\alpha_2}{5!} + \frac{\beta_2}{4!} + \frac{\omega_2}{3!} + \frac{\gamma_2}{6!}\right) = 0, \\ y_{24} = 2\left(\frac{\alpha_2}{7!} + \frac{\beta_2}{6!} + \frac{\omega_2}{5!} + \frac{\gamma_2}{8!}\right) = 0, \end{cases} \tag{18}$$

and

$$\begin{cases} y_{31} = 2(\alpha_3 + \gamma_3) = 0, \\ y_{32} = 2\left(\frac{\alpha_3}{2!} + \beta_3 + \omega_3 + \frac{\gamma_3}{3!}\right) + 1 = 0, \\ y_{33} = 2\left(\frac{\alpha_3}{4!} + \frac{\beta_3}{3!} + \frac{\omega_3}{2!} + \frac{\gamma_3}{5!}\right) = 0, \\ y_{34} = 2\left(\frac{\alpha_3}{6!} + \frac{\beta_3}{5!} + \frac{\omega_3}{4!} + \frac{\gamma_3}{7!}\right) = 0. \end{cases} \tag{19}$$

Table 4. Taylor series of scheme (15).

Term	$u_j h^{-2}$	$u_j' h$	u_j''	$u_j''' h$	$u_j^{(4)} h^2$	$u_j^{(5)} h^3$	$u_j^{(6)} h^4$	$u_j^{(7)} h^5$	$u_j^{(8)} h^6$
$\frac{\alpha_2}{h} u_{j+1}'$	0	α_2	α_2	$\frac{\alpha_2}{2!}$	$\frac{\alpha_2}{3!}$	$\frac{\alpha_2}{4!}$	$\frac{\alpha_2}{5!}$	$\frac{\alpha_2}{6!}$	$\frac{\alpha_2}{7!}$
$-\frac{\alpha_2}{h} u_{j-1}'$	0	$-\alpha_2$	α_2	$-\frac{\alpha_2}{2!}$	$\frac{\alpha_2}{3!}$	$-\frac{\alpha_2}{4!}$	$\frac{\alpha_2}{5!}$	$-\frac{\alpha_2}{6!}$	$\frac{\alpha_2}{7!}$
u_j''	0	0	1	0	0	0	0	0	0
$\beta_2 u_{j+1}''$	0	0	β_2	β_2	$\frac{\beta_2}{2!}$	$\frac{\beta_2}{3!}$	$\frac{\beta_2}{4!}$	$\frac{\beta_2}{5!}$	$\frac{\beta_2}{6!}$
$\beta_2 u_{j-1}''$	0	0	β_2	$-\beta_2$	$\frac{\beta_2}{2!}$	$-\frac{\beta_2}{3!}$	$\frac{\beta_2}{4!}$	$-\frac{\beta_2}{5!}$	$\frac{\beta_2}{6!}$
$\omega_2 u_{j+1}''' h$	0	0	0	ω_2	ω_2	$\frac{\omega_2}{2!}$	$\frac{\omega_2}{3!}$	$\frac{\omega_2}{4!}$	$\frac{\omega_2}{5!}$
$-\omega_2 u_{j-1}''' h$	0	0	0	$-\omega_2$	ω_2	$-\frac{\omega_2}{2!}$	$\frac{\omega_2}{3!}$	$-\frac{\omega_2}{4!}$	$\frac{\omega_2}{5!}$
$\frac{\gamma_2}{h^2} u_{j+1}$	γ_2	γ_2	$\frac{\gamma_2}{2!}$	$\frac{\gamma_2}{3!}$	$\frac{\gamma_2}{4!}$	$\frac{\gamma_2}{5!}$	$\frac{\gamma_2}{6!}$	$\frac{\gamma_2}{7!}$	$\frac{\gamma_2}{8!}$
$-\frac{2\gamma_2}{h^2} u_j$	$-2\gamma_2$	0	0	0	0	0	0	0	0
$\frac{\gamma_2}{h^2} u_{j-1}$	γ_2	$-\gamma_2$	$\frac{\gamma_2}{2!}$	$-\frac{\gamma_2}{3!}$	$\frac{\gamma_2}{4!}$	$-\frac{\gamma_2}{5!}$	$\frac{\gamma_2}{6!}$	$-\frac{\gamma_2}{7!}$	$\frac{\gamma_2}{8!}$
Σ	0	0	y_{21}	0	y_{22}	0	y_{23}	0	y_{24}

Table 5. Taylor series of scheme (16).

Term	$u_j h^{-3}$	$u_j' h^{-2}$	$u_j'' h^{-1}$	u_j'''	$u_j^{(4)} h$	$u_j^{(5)} h^2$	$u_j^{(6)} h^3$	$u_j^{(7)} h^4$	$u_j^{(8)} h^5$
$\frac{\alpha_3}{h^2} u_{j+1}'$	0	α_3	α_3	$\frac{\alpha_3}{2!}$	$\frac{\alpha_3}{3!}$	$\frac{\alpha_3}{4!}$	$\frac{\alpha_3}{5!}$	$\frac{\alpha_3}{6!}$	$\frac{\alpha_3}{7!}$
$\frac{\alpha_3}{h^2} u_{j-1}'$	0	α_3	$-\alpha_3$	$\frac{\alpha_3}{2!}$	$-\frac{\alpha_3}{3!}$	$\frac{\alpha_3}{4!}$	$-\frac{\alpha_3}{5!}$	$\frac{\alpha_3}{6!}$	$-\frac{\alpha_3}{7!}$
u_j'''	0	0	0	1	0	0	0	0	0
$\frac{\beta_3}{h} u_{j+1}''$	0	0	β_3	β_3	$\frac{\beta_3}{2!}$	$\frac{\beta_3}{3!}$	$\frac{\beta_3}{4!}$	$\frac{\beta_3}{5!}$	$\frac{\beta_3}{6!}$
$-\frac{\beta_3}{h} u_{j-1}''$	0	0	$-\beta_3$	β_3	$-\frac{\beta_3}{2!}$	$\frac{\beta_3}{3!}$	$-\frac{\beta_3}{4!}$	$\frac{\beta_3}{5!}$	$-\frac{\beta_3}{6!}$
$\omega_3 u_{j+1}'''$	0	0	0	ω_3	ω_3	$\frac{\omega_3}{2!}$	$\frac{\omega_3}{3!}$	$\frac{\omega_3}{4!}$	$\frac{\omega_3}{5!}$
$\omega_3 u_{j-1}'''$	0	0	0	ω_3	$-\omega_3$	$\frac{\omega_3}{2!}$	$-\frac{\omega_3}{3!}$	$\frac{\omega_3}{4!}$	$-\frac{\omega_3}{5!}$
$\frac{\gamma_3}{h^3} u_{j+1}$	γ_3	γ_3	$\frac{\gamma_3}{2!}$	$\frac{\gamma_3}{3!}$	$\frac{\gamma_3}{4!}$	$\frac{\gamma_3}{5!}$	$\frac{\gamma_3}{6!}$	$\frac{\gamma_3}{7!}$	$\frac{\gamma_3}{8!}$
$-\frac{\gamma_3}{h^3} u_{j-1}$	$-\gamma_3$	γ_3	$-\frac{\gamma_3}{2!}$	$\frac{\gamma_3}{3!}$	$-\frac{\gamma_3}{4!}$	$\frac{\gamma_3}{5!}$	$-\frac{\gamma_3}{6!}$	$\frac{\gamma_3}{7!}$	$-\frac{\gamma_3}{8!}$
Σ	0	y_{31}	0	y_{32}	0	y_{33}	0	y_{34}	0

Their unique solutions are

$$\alpha_1 = \frac{19}{32}, \beta_1 = -\frac{1}{8}, \omega_1 = \frac{1}{96}, \gamma_1 = -\frac{35}{32}$$

and

$$\alpha_2 = \frac{29}{16}, \beta_2 = -\frac{5}{16}, \omega_2 = \frac{1}{48}, \gamma_2 = -4$$

and

$$\alpha_3 = -\frac{105}{16}, \beta_3 = \frac{15}{8}, \omega_3 = -\frac{3}{16}, \gamma_3 = \frac{105}{16}$$

respectively. Therefore, schemes (14)–(16) have the following specific forms:

$$\frac{1}{32}\left(19u'_{j+1} + 32u'_j + 19u'_{j-1}\right) - \frac{h}{8}\left(u''_{j+1} - u''_{j-1}\right) + \frac{h^2}{96}\left(u'''_{j+1} + u'''_{j-1}\right) = \frac{35}{32h}\left(u_{j+1} - u_{j-1}\right), \tag{20}$$

$$\frac{\left(29u'_{j+1} - 29u'_{j-1}\right)}{16h} - \frac{\left(5u''_{j+1} - 16u''_j + 5u''_{j-1}\right)}{16} + \frac{h\left(u'''_{j+1} - u'''_{j-1}\right)}{48} = \frac{4\left(u_{j+1} - 2u_j + u_{j-1}\right)}{h^2}, \tag{21}$$

$$\frac{\left(105u'_{j+1} + 105u'_{j-1}\right)}{-16h^2} + \frac{\left(15u''_{j+1} - 15u''_{j-1}\right)}{8h} - \frac{\left(3u'''_{j+1} - 16u'''_j + 3u'''_{j-1}\right)}{16} = \frac{105\left(u_{j+1} - u_{j-1}\right)}{-16h^3}. \tag{22}$$

This three-point scheme possesses eighth-order accuracy and involves three derivatives, so it is more applicable and allows for greater accuracy in comparison to (4) and (5). Under periodic boundary conditions, by combining (20)–(22), we have

$$\begin{cases} \mathrm{B}_{11}U_x + \mathrm{B}_{12}U_{xx} + \mathrm{B}_{13}U_{xxx} = \mathrm{B}_{14}U, \\ \mathrm{B}_{21}U_x + \mathrm{B}_{22}U_{xx} + \mathrm{B}_{23}U_{xxx} = \mathrm{B}_{24}U, \\ \mathrm{B}_{31}U_x + \mathrm{B}_{32}U_{xx} + \mathrm{B}_{33}U_{xxx} = \mathrm{B}_{34}U. \end{cases} \tag{23}$$

where

$$\mathrm{B}_{11} = \frac{19}{32}\begin{bmatrix} \frac{32}{19} & 1 & & & 1 \\ 1 & \frac{32}{19} & 1 & & \\ & \ddots & \ddots & \ddots & \\ & & 1 & \frac{32}{19} & 1 \\ 1 & & & 1 & \frac{32}{19} \end{bmatrix}, \mathrm{B}_{12} = -\frac{h}{8}\begin{bmatrix} 0 & 1 & & & -1 \\ -1 & 0 & 1 & & \\ & \ddots & \ddots & \ddots & \\ & & -1 & 0 & 1 \\ 1 & & & -1 & 0 \end{bmatrix}, \mathrm{B}_{13} = \frac{h^2}{96}\begin{bmatrix} 0 & 1 & & & 1 \\ 1 & 0 & 1 & & \\ & \ddots & \ddots & \ddots & \\ & & 1 & 0 & 1 \\ 1 & & & 1 & 0 \end{bmatrix},$$

$$\mathrm{B}_{14} = \frac{35}{32h}\begin{bmatrix} 0 & 1 & & & -1 \\ -1 & 0 & 1 & & \\ & \ddots & \ddots & \ddots & \\ & & -1 & 0 & 1 \\ 1 & & & -1 & 0 \end{bmatrix}, \mathrm{B}_{21} = \frac{29}{16h}\begin{bmatrix} 0 & 1 & & & -1 \\ -1 & 0 & 1 & & \\ & \ddots & \ddots & \ddots & \\ & & -1 & 0 & 1 \\ 1 & & & -1 & 0 \end{bmatrix}, \mathrm{B}_{22} = -\frac{5}{16}\begin{bmatrix} -\frac{16}{5} & 1 & & & 1 \\ 1 & -\frac{16}{5} & 1 & & \\ & \ddots & \ddots & \ddots & \\ & & 1 & -\frac{16}{5} & 1 \\ 1 & & & 1 & -\frac{16}{5} \end{bmatrix},$$

$$\mathrm{B}_{23} = \frac{h}{48}\begin{bmatrix} 0 & 1 & & & -1 \\ -1 & 0 & 1 & & \\ & \ddots & \ddots & \ddots & \\ & & -1 & 0 & 1 \\ 1 & & & -1 & 0 \end{bmatrix}, \mathrm{B}_{24} = \frac{4}{h^2}\begin{bmatrix} -2 & 1 & & & 1 \\ 1 & -2 & 1 & & \\ & \ddots & \ddots & \ddots & \\ & & 1 & -2 & 1 \\ 1 & & & 1 & -2 \end{bmatrix}, \mathrm{B}_{31} = -\frac{105}{16h^2}\begin{bmatrix} 0 & 1 & & & -1 \\ -1 & 0 & 1 & & \\ & \ddots & \ddots & \ddots & \\ & & -1 & 0 & 1 \\ 1 & & & -1 & 0 \end{bmatrix},$$

$$\mathrm{B}_{32} = \frac{15}{8h}\begin{bmatrix} 0 & 1 & & & -1 \\ -1 & 0 & 1 & & \\ & \ddots & \ddots & \ddots & \\ & & -1 & 0 & 1 \\ 1 & & & -1 & 0 \end{bmatrix}, \mathrm{B}_{33} = -\frac{3}{16}\begin{bmatrix} -\frac{16}{3} & 1 & & & 1 \\ 1 & -\frac{16}{3} & 1 & & \\ & \ddots & \ddots & \ddots & \\ & & 1 & -\frac{16}{3} & 1 \\ 1 & & & 1 & -\frac{16}{3} \end{bmatrix}, \mathrm{B}_{34} = -\frac{105}{16h^3}\begin{bmatrix} 0 & 1 & & & -1 \\ -1 & 0 & 1 & & \\ & \ddots & \ddots & \ddots & \\ & & -1 & 0 & 1 \\ 1 & & & -1 & 0 \end{bmatrix}.$$

Next, we adopt the combination of the function values of u and its first, second, and third derivatives to represent the fourth-order spatial derivative

$$u_j^{(4)} = -\frac{72}{h^4}(u_{j+1} - 2u_j + u_{j-1}) + \frac{183}{4h^3}\left(u'_{j+1} - u'_{j-1}\right) - \frac{39}{4h^2}\left(u''_{j+1} + u''_{j-1}\right) + \frac{3}{4h}\left(u'''_{j+1} - u'''_{j-1}\right). \tag{24}$$

In light of solving (23), we can obtain

$$\begin{cases} \partial_x U = \mathrm{G}^* \cdot U, \\ \partial_x^2 U = \mathrm{H}^* \cdot U, \\ \partial_x^3 U = \mathrm{I} \cdot U, \end{cases} \tag{25}$$

where $\mathrm{G}^* = \mathrm{D}^{-1}\mathrm{D}_1, \mathrm{H}^* = \mathrm{D}^{-1}\mathrm{D}_2, \mathrm{I} = \mathrm{D}^{-1}\mathrm{D}_3$. For $\mathrm{D}, \mathrm{D}_1, \mathrm{D}_2$ and D_3, we have

$$\begin{cases} \mathrm{D} = \mathrm{B}_{11}\mathrm{B}_{22}\mathrm{B}_{33} + \mathrm{B}_{12}\mathrm{B}_{23}\mathrm{B}_{31} + \mathrm{B}_{13}\mathrm{B}_{21}\mathrm{B}_{32} - \mathrm{B}_{11}\mathrm{B}_{23}\mathrm{B}_{32} - \mathrm{B}_{12}\mathrm{B}_{21}\mathrm{B}_{33} - \mathrm{B}_{13}\mathrm{B}_{22}\mathrm{B}_{31}, \\ \mathrm{D}_1 = \mathrm{B}_{14}\mathrm{B}_{22}\mathrm{B}_{33} + \mathrm{B}_{14}\mathrm{B}_{23}\mathrm{B}_{31} + \mathrm{B}_{13}\mathrm{B}_{21}\mathrm{B}_{34} - \mathrm{B}_{11}\mathrm{B}_{23}\mathrm{B}_{34} - \mathrm{B}_{14}\mathrm{B}_{21}\mathrm{B}_{33} - \mathrm{B}_{13}\mathrm{B}_{24}\mathrm{B}_{31}, \\ \mathrm{D}_2 = \mathrm{B}_{11}\mathrm{B}_{22}\mathrm{B}_{34} + \mathrm{B}_{12}\mathrm{B}_{24}\mathrm{B}_{31} + \mathrm{B}_{14}\mathrm{B}_{21}\mathrm{B}_{32} - \mathrm{B}_{13}\mathrm{B}_{24}\mathrm{B}_{31} - \mathrm{B}_{14}\mathrm{B}_{21}\mathrm{B}_{33} - \mathrm{B}_{11}\mathrm{B}_{23}\mathrm{B}_{34}, \\ \mathrm{D}_3 = \mathrm{B}_{11}\mathrm{B}_{22}\mathrm{B}_{34} + \mathrm{B}_{12}\mathrm{B}_{24}\mathrm{B}_{31} + \mathrm{B}_{14}\mathrm{B}_{21}\mathrm{B}_{32} - \mathrm{B}_{11}\mathrm{B}_{24}\mathrm{B}_{32} - \mathrm{B}_{12}\mathrm{B}_{21}\mathrm{B}_{34} - \mathrm{B}_{14}\mathrm{B}_{22}\mathrm{B}_{31}. \end{cases} \tag{26}$$

Substituting $U_x = \mathrm{G}^* \cdot U, U_{xx} = \mathrm{H}^* \cdot U, U_{xxx} = \mathrm{I} \cdot U$ into (24) gives

$$\partial_x^4 U = -\frac{18}{\mathrm{h}^2}\mathrm{B}_{24} \cdot U - \frac{366}{h^4}\mathrm{B}_{12}\mathrm{G}^* \cdot U + \frac{936}{h^4}\mathrm{B}_{13}\mathrm{H}^* \cdot U - \frac{6}{h^2}\mathrm{B}_{12}\mathrm{I} \cdot U. \tag{27}$$

Let $\mathrm{M}^* = \frac{936}{h^4}\mathrm{B}_{13}\mathrm{H}^* - \frac{366}{h^4}\mathrm{B}_{12}\mathrm{G}^* - \frac{18}{h^2}\mathrm{B}_{24} - \frac{6}{h^2}\mathrm{B}_{12}\mathrm{I}$. We will obtain the following discrete schemes of the spatial derivative, as follows:

$$\begin{cases} \partial_x^4 U = \mathrm{M}^* \cdot U, \\ \partial_x^2 U = \mathrm{H}^* \cdot U. \end{cases} \tag{28}$$

For the above scheme, we find that the matrix operation becomes complicated. To obtain the discrete form of $\partial_x^2 u$ and $\partial_x^4 u$ according to (14)–(16), we require many matrix operations, and the subsequent simulation of the numerical solution will be more difficult. Thus, we consider constructing a direct combination of $\partial_x^2 u, \partial_x^4 u$ and u to devise the third CHOC scheme. This scheme will maintain sixth-order precision and can be used to easily obtain the discrete forms of $\partial_x^2 u$ and $\partial_x^4 u$, which will be more pertinent and accurate. This scheme has the following formulation:

$$\alpha_1\left(\frac{u''_{j+1} + u''_{j-1}}{2}\right) + u''_j + \beta_1 h^2\left(\frac{u_{j+1}^{(4)} + u_{j-1}^{(4)}}{2}\right) = \gamma_1\frac{u_{j+1} - 2u_j + u_{j-1}}{h^2}, \tag{29}$$

$$\alpha_2\left(\frac{u''_{j+1} - 2u''_j + u''_{j-1}}{h^2}\right) + u_j^{(4)} + \beta_2\left(\frac{u_{j+1}^{(4)} + u_{j-1}^{(4)}}{2}\right) = \gamma_2\frac{u_{j+2} - 4u_{j+1} + 6u_j - 4u_{j-1} + u_{j-2}}{h^4}. \tag{30}$$

We apply Taylor expansion to (29) to obtain

$$\begin{aligned}
LHS &= u_j'' + \alpha_1\left(\frac{u_{j+1}'' + u_{j-1}''}{2}\right) + \beta_1 h^2\left(\frac{u_{j+1}^{(4)} + u_{j-1}^{(4)}}{2}\right)\\
&= u_j'' + \alpha_1\left(u_j'' + \frac{h^2}{2!}u_j^{(4)} + \frac{h^4}{4!}u_j^{(6)} + o\left(h^6\right)\right) + \beta_1 h^2\left(u_j^{(4)} + \frac{h^2}{2!}u_j^{(6)} + \frac{h^4}{4!}u_j^{(8)} + o\left(h^6\right)\right)\\
&= (1+\alpha_1)u_j'' + \left(\frac{\alpha_1}{2!} + \beta_1\right)h^2 u_j^{(4)} + \left(\frac{\alpha_1}{4!} + \frac{\beta_1}{2!}\right)h^4 u_j^{(6)} + o\left(h^6\right),\\
RHS &= \gamma_1\left(\frac{u_{j+1} - 2u_j + u_{j-1}}{h^2}\right)\\
&= \gamma_1\left(u_j'' + \frac{u_j^{(4)}}{12}h^2 + \frac{u_j^{(6)}}{360}h^4\right) + o\left(h^6\right).
\end{aligned}$$

To obtain the scheme with sixth-order accuracy, the coefficients must satisfy the algebraic equations

$$\begin{cases} 1 + \alpha_1 = \frac{\gamma_1}{2!}, \\ \frac{\alpha_1}{2!} + \beta_1 = \frac{\gamma_1}{4!}, \\ \frac{\alpha_1}{4!} + \frac{\beta_1}{2!} = \frac{\gamma_1}{6!}, \end{cases} \Rightarrow \begin{cases} \alpha_1 = \frac{14}{61}, \\ \beta_1 = -\frac{3}{244}, \\ \gamma_1 = \frac{75}{61}. \end{cases}$$

Similarly, for (30), we have

$$\begin{aligned}
LHS &= u_j^{(4)} + \alpha_2\left(u_j^{(4)} + \frac{u_j^{(6)}}{12}h^2 + \frac{u_j^{(8)}}{360}h^4\right) + \beta_2\left(u_j^{(4)} + \frac{u_j^{(6)}h^2}{2!} + \frac{u_j^{(8)}h^4}{4!}\right) + o\left(h^6\right)\\
&= (1+\alpha_2+\beta_2)u_j^{(4)} + \left(\frac{\alpha_2}{12} + \frac{\beta_2}{2!}\right)h^2 u_j^{(6)} + \left(\frac{\alpha_2}{360} + \frac{\beta_2}{4!}\right)h^4 u_j^{(8)} + o\left(h^6\right),\\
RHS &= \gamma_2\frac{u_{j+2} - 4u_{j+1} + 6u_j - 4u_{j-1} + u_{j-2}}{h^4} + o\left(h^6\right)\\
&= \gamma_2\left(\frac{2^5 - 2^3}{4!}u_j^{(4)} + \frac{2^7 - 2^3}{6!}h^2 u_j^{(6)} + \frac{2^9 - 2^3}{8!}h^4 u_j^{(8)}\right) + o\left(h^6\right).
\end{aligned}$$

To obtain the scheme with sixth-order accuracy, the coefficients must satisfy the algebraic equations

$$\begin{cases} 1 + \alpha_2 + \beta_2 = \frac{2^5-2^3}{4!}\gamma_2, \\ \frac{\alpha_2}{12} + \frac{\beta_2}{2!} = \frac{2^7-2^3}{6!}\gamma_2, \\ \frac{\alpha_2}{360} + \frac{\beta_2}{4!} = \frac{2^9-2^3}{8!}\gamma_2, \end{cases} \Longrightarrow \begin{cases} \alpha_2 = \frac{6}{7}, \\ \beta_2 = \frac{5}{7}, \\ \gamma_2 = \frac{18}{7}. \end{cases}$$

Under periodic boundary conditions, for (29) and (30), we obtain

$$\begin{cases} \mathrm{A}_{11}^* U_{xx} + \mathrm{A}_{12}^* U_{xxxx} = \mathrm{A}_{13}^* U, \\ \mathrm{A}_{21}^* U_{xx} + \mathrm{A}_{22}^* U_{xxxx} = \mathrm{A}_{23}^* U. \end{cases} \tag{31}$$

where

$$\mathrm{A}_{11}^{*}=\frac{7}{61}\begin{bmatrix}\frac{61}{7} & 1 & & & 1\\ 1 & \frac{61}{7} & 1 & & \\ & \ddots & \ddots & \ddots & \\ & & 1 & \frac{61}{7} & 1\\ 1 & & & 1 & \frac{61}{7}\end{bmatrix},\mathrm{A}_{12}^{*}=-\frac{3h^2}{488}\begin{bmatrix}0 & 1 & & & 1\\ 1 & 0 & 1 & & \\ & \ddots & \ddots & \ddots & \\ & & 1 & 0 & 1\\ 1 & & & 1 & 0\end{bmatrix},\mathrm{A}_{13}^{*}=\frac{75}{61h^2}\begin{bmatrix}-2 & 1 & & & 1\\ 1 & -2 & 1 & & \\ & \ddots & \ddots & \ddots & \\ & & 1 & -2 & 1\\ 1 & & & 1 & -2\end{bmatrix},$$

$$\mathrm{A}_{21}^{*}=\frac{6}{7h^2}\begin{bmatrix}-2 & 1 & & & 1\\ 1 & -2 & 1 & & \\ & \ddots & \ddots & \ddots & \\ & & 1 & -2 & 1\\ 1 & & & 1 & -2\end{bmatrix},\mathrm{A}_{22}^{*}=\frac{5}{14}\begin{bmatrix}\frac{14}{5} & 1 & & & 1\\ 1 & \frac{14}{5} & 1 & & \\ & \ddots & \ddots & \ddots & \\ & & 1 & \frac{14}{5} & 1\\ 1 & & & 1 & \frac{14}{5}\end{bmatrix},\mathrm{A}_{23}^{*}=\frac{18}{7h^4}\begin{bmatrix}6 & -4 & 1 & & & & 1 & -4\\ -4 & 6 & -4 & 1 & & & & 1\\ 1 & -4 & 6 & -4 & 1 & & & \\ & \ddots & \ddots & \ddots & \ddots & \ddots & & \\ & & \ddots & \ddots & \ddots & \ddots & \ddots & \\ & & & \ddots & \ddots & \ddots & \ddots & 1\\ 1 & & & & 1 & -4 & 6 & -4\\ -4 & 1 & & & & 1 & -4 & 6\end{bmatrix}.$$

With (31), we can readily derive U_{xx} and U_{xxxx} via the expressions of U. This significantly streamlines the matrix operations. By solving (31), we can obtain

$$\begin{cases}\partial_x^2 U=\mathrm{G}_1\cdot U,\\ \partial_x^4 U=\mathrm{H}_1\cdot U.\end{cases}\tag{32}$$

where $\mathrm{G}_1=\mathrm{A}_1^{-1}\mathrm{B}_1,\mathrm{H}_1=\mathrm{A}_1^{-1}\mathrm{C}_1$. For $\mathrm{A}_1,\mathrm{B}_1,\mathrm{C}_1$, we have

$$\begin{cases}\mathrm{A}_1=\mathrm{A}_{11}^{*}\mathrm{A}_{22}^{*}-\mathrm{A}_{12}^{*}\mathrm{A}_{21}^{*},\\ \mathrm{B}_1=\mathrm{A}_{22}^{*}\mathrm{A}_{13}^{*}-\mathrm{A}_{12}^{*}\mathrm{A}_{23}^{*},\\ \mathrm{C}_1=\mathrm{A}_{11}^{*}\mathrm{A}_{23}^{*}-\mathrm{A}_{21}^{*}\mathrm{A}_{13}^{*}.\end{cases}\tag{33}$$

Additionally, the following high-order compact (HOC) scheme is presented in the existing literature [28]. For good Boussinesq equations, the above scheme has higher spatial accuracy compared to the scheme given in [28].

$$\alpha_1 u_{j-1}''+u_j''+\alpha_1 u_{j+1}''=b_1\frac{u_{j+2}-2u_j+u_{j-2}}{4h^2}+a_1\frac{u_{j+1}-2u_j+u_{j-1}}{h^2},\tag{34}$$

$$\begin{aligned}\alpha_2 u_{j-1}^{(4)}+u_j^{(4)}+\alpha_2 u_{j+1}^{(4)} &= b_2\tfrac{u_{j+3}-9u_{j+1}+16u_j-9u_{j-1}+u_{j-3}}{6h^4}\\ &+a_2\tfrac{u_{j+2}-4u_{j+1}+6u_j-4u_{j-1}+u_{j-2}}{h^4},\end{aligned}\tag{35}$$

for (34) and (35), according to [28], we have $\alpha_1=\frac{2}{11}$, $\alpha_2=\frac{7}{26}$, $a_1=\frac{12}{11}$, $a_2=\frac{19}{13}$, $b_1=\frac{3}{11}$, $b_2=\frac{1}{13}$. Therefore, we can also express this HOC scheme in the same way as in the three aforementioned schemes, where we denote

$$\begin{cases}\partial_x^4 U=\mathrm{S}_2\cdot U,\\ \partial_x^2 U=\mathrm{S}_1\cdot U.\end{cases}\tag{36}$$

3. Establishment of the Fully Discrete Scheme

Let τ be a temporal step size and $t_n = n\tau, n = 0, 1, 2, \cdots, M$, where $M = T/\tau$. Denote the approximation of $u(x, t_n)$ by u^n. Define the following operators:

$$\delta_t u^{n+\frac{1}{2}} = \frac{u^{n+1} - u^n}{\tau}, \quad u^{n+\frac{1}{2}} = \frac{u^n + u^{n+1}}{2}.$$

Let $v = u_t$, and the considered good Boussinesq equation can be written as

$$\partial_t v = \partial_x^2 u - \partial_x^4 u + \partial_x^2 (u^2).$$

Applying the CHOC scheme (13) to the spatial derivatives of the above equation gives

$$v_t = -M \cdot u + H \cdot u + H \cdot u^2 = N \cdot u + H \cdot u^2,$$

where $N = H - M$. By applying a symplectic midpoint scheme with second-order accuracy to the above equation, we obtain the following fully discrete scheme:

$$u^{n+1} = u^n + \frac{\tau}{2}\left(v^n + v^{n+1}\right), \tag{37}$$

$$-\frac{\tau}{2} N \cdot u^{n+1} + v^{n+1} = \frac{\tau}{2} N \cdot u^n + v^n + \frac{\tau}{2} H \cdot \left\{ \left(u^2\right)^n + \left(u^2\right)^{n+1} \right\}. \tag{38}$$

Similarly, using CHOC scheme (28) for the spatial derivatives yields

$$v_t = -M^* \cdot u + H^* \cdot u + H^* \cdot u^2 = N^* \cdot u + H^* \cdot u^2,$$

where $N^* = H^* - M^*$. We obtain the corresponding fully discrete scheme

$$-\frac{\tau}{2} N^* \cdot u^{n+1} + v^{n+1} = \frac{\tau}{2} N^* \cdot u^n + v^n + \frac{\tau}{2} H^* \cdot \left\{ \left(u^2\right)^n + \left(u^2\right)^{n+1} \right\}. \tag{39}$$

Applying the CHOC scheme (31) for the spatial derivatives gives

$$v_t = -H_1 \cdot u + G_1 \cdot u + G_1 \cdot u^2 = N_1 \cdot u + G_1 \cdot u^2,$$

where $N_1 = G_1 - H_1$. We similarly obtain the following fully discrete scheme:

$$-\frac{\tau}{2} N_1 \cdot u^{n+1} + v^{n+1} = \frac{\tau}{2} N_1 \cdot u^n + v^n + \frac{\tau}{2} G_1 \cdot \left\{ \left(u^2\right)^n + \left(u^2\right)^{n+1} \right\}. \tag{40}$$

Applying the HOC scheme (34) and (35) for the spatial derivatives gives

$$v_t = -S_2 \cdot u + S_1 \cdot u + S_1 \cdot u^2 = S_3 \cdot u + S_1 \cdot u^2,$$

where $S_3 = S_1 - S_2$. We also similarly obtain the following fully discrete scheme:

$$-\frac{\tau}{2} S_3 \cdot u^{n+1} + v^{n+1} = \frac{\tau}{2} S_3 \cdot u^n + v^n + \frac{\tau}{2} S_1 \cdot \left\{ \left(u^2\right)^n + \left(u^2\right)^{n+1} \right\}. \tag{41}$$

By combining (38)–(41) with (37), respectively, we always obtain the algebraic equation as follows:

$$A \cdot T^{n+1} = B \cdot T^n + F\left(T^{n+1}, T^n\right),$$

where A and B are some invertible tridiagonal matrices depending on the corresponding scheme, $T^n = [u^n, v^n]^\intercal$, and F is the corresponding nonlinear term.

For simplicity, we will denote the schemes corresponding to (38)–(41) by CHOC-A, CHOC-B, CHOC-C, and HOC, respectively.

4. Conservation Laws of CHOC Schemes

Under periodic boundary condition (3) with $L = 1$, some good Boussinesq equations have certain conservation laws. Below, we consider periodic domain $[0, 1]$.

Theorem 1. *Let $\|\cdot\|$ denote the standard L^2-norm for 1-periodic functions. Then, along with $\partial_t^2 u = -\partial_x^4 u$, the quadratic functional*

$$\|u_t\|^2 + \|u_{xx}\|^2 \tag{42}$$

is invariant. Thus, it is an integral of motion.

Proof. According to (3), after multiplying both sides of $\partial_t^2 u = -\partial_x^4 u$ by u_t and integrating it by parts, we have

$$\int_0^1 u_t \cdot u_{tt} dx = -\int_0^1 u_{xx} \cdot u_{txx} dx. \tag{43}$$

For (43), we take integration with respect to t to obtain

$$\int_0^t \int_0^1 u_t \cdot u_{tt}\, dx\, dt = -\int_0^t \int_0^1 u_{xx} u_{txx}\, dx\, dt.$$

$$\Rightarrow \int_0^1 u_t^2(x,t)\, dx + \int_0^1 u_{xx}^2(x,t)\, dx = \int_0^1 u_t^2(x,0)\, dx + \int_0^1 u_{xx}^2(x,0)\, dx.$$

Therefore, we have (42). □

Theorem 2. *For nonlinear Boussinesq Equation (2), the following conservation law is satisfied:*

$$\int_0^1 u_t(x,t)\, dx = \int_0^1 v^0(x)\, dx. \tag{44}$$

If $\int_0^1 v^0(x)\, dx = 0$, then we obtain the conservation law as follows:

$$\int_0^1 u(x,t)\, dx = \int_0^1 u^0(x)\, dx. \tag{45}$$

Proof. For $t \in [0, T]$, integrating with respect to x on both sides of (2), we obtain

$$\int_0^1 u_{tt} dx = \int_0^1 (u_{xx} - \partial_x^4 u + (u^2)_{xx}) dx.$$

According to (3), the integration on the right side of the above equation is 0, i.e.,

$$\int_0^1 u_{tt} dx = 0.$$

Taking integration with respect to t yields $\int_0^1 u_t(x,t) dx = \int_0^1 v^0(x) dx$, which is (44). If $\int_0^1 v^0(x)\, dx = 0$, then $\int_0^1 u_t(x,t) dx = 0$, which gives (45) by integration with respect to t.

First, we are interested in the discrete versions of Theorems 1 and 2 under numerical analysis for CHOC schemes. To this end, we list some important properties of circulant matrices [11]. A matrix written in the form

$$Circ(c_0, c_1, c_2 \cdots c_{N-1}) = \begin{bmatrix} c_0 & c_1 & c_2 & \cdots & c_{N-1} \\ c_{N-1} & c_0 & c_1 & \cdots & c_{N-2} \\ \cdots & \ddots & \ddots & \ddots & \cdots \\ c_2 & c_3 & \ddots & \ddots & c_1 \\ c_1 & c_2 & \cdots & c_{N-1} & c_0 \end{bmatrix}$$

is said to be a circulant matrix.

All of the matrices $A_{ij}(i,j=1,2.)$, $B_{ij}(i,j=1,2,3.)$, $A^*_{ij}(i,j=1,2.)$ are circulant. There are a number of favorable characteristics of this type of matrix.

We list some of them in the following; these are useful in analyzing our schemes. □

Proposition 1 ([11,27]). *If A, B are circulant matrices with the same number of rows and columns, then we have the following.*

(i) $A+B$, $A-B$, AB *are circulant matrices.*
(ii) *If* A^{-1} *is well defined, then* A^{-1} *is also a circulant matrix.*
(iii) A, B *are commutators,* $AB = BA$.
(iv) *If* A, B *are symmetric and positive definite matrices, then* $AB = BA$ *is a symmetric and positive definite matrix.*
(v) *The eigenvalue of the circulant matrix above is* $\lambda_j = \sum_{k=0}^{N-1} c_k e^{-ik\theta_j}$ *with the corresponding eigenvector* $w_j = \frac{1}{N}\left[1, e^{-i\theta_j}, \cdots, e^{-i(N-1)\theta_j}\right]^\intercal$.

With Proposition 1, we can obtain the following proposition.

Proposition 2. *For the matrices in the CHOC solvers (13), (28), (31), and the HOC solver (36), we have the following:*

(i) A_{11}, A_{22}, $-A_{23}$, B_{22}, B_{33}, A^*_{11}, A^*_{22}, A^*_{23} *are symmetric and positive definite.*
(ii) A_{12}, A_{13}, A_{21}, B_{12}, B_{14}, B_{21}, B_{23}, B_{34} *are skew-symmetric.*
(iii) B_{11}, B_{13}, B_{24}, B_{31}, B_{32}, A^*_{12}, A^*_{13}, A^*_{21}, S_1 *are symmetric.*
(iv) A, A^{-1}, D, A_1, C_1 *are symmetric and positive definite;* D_1, D_3 *are skew-symmetric; and* D_2, B_1 *are symmetric.*
(v) M^*, H_1, S_2 *are symmetric and positive definite;* G, G^*, I, *are skew-symmetric; and* H, M, H^*, G_1, N, N^*, N_1, S_1 *are symmetric.*
(vi) *All of these are circulant.*

Proof. The conclusions (i)–(iv) and (vi) can be observed or be verified from Proposition 1. The result (v) can be derived from the last conclusion in Proposition 1 by finding their eigenvalues. □

Theorem 3. *Define*

$$w^n = (v^n, v^n) + (u^n, R \cdot u^n),$$

where (u,v) *is the standard unitary inner product at the discrete level for finite-dimensional sequence vectors,* $v^n = \left[v_1^n, v_2^n, \cdots, v_{NX}^n\right]^\intercal$, $u^n = \left[u_1^n, u_2^n, \cdots, u_{NX}^n\right]^\intercal$. R *is the matrix coefficient when approximating the fourth-order spatial derivative expressed by* M *(13),* M^* *(28),* H_1 *(31),* S_2 *(36). Then, for CHOC solvers (13), (28), (31), and HOC solver (36) to solve* $\partial_t^2 u = -\partial_x^4 u$, *the numerical solutions satisfy that*

$$\omega^{n+1} = w^n. \tag{46}$$

Moreover, for M^* *(28),* H_1 *(31) and* S_2 *(36), there exists* C *such that* $C^\intercal \cdot C = R$; *therefore,*

$$w^n = (v^n, v^n) + (C \cdot u^n, C \cdot u^n).$$

Proof. Since $v = u_t$, we have $v_t = -u_{xxxx}$, and its discrete scheme is

$$\frac{v^{n+1} - v^n}{\tau} = -\frac{Ru^{n+1} + Ru^n}{2}.$$

By multiplying $\frac{u^{n+1}-u^n}{\tau} = \frac{v^{n+1}+v^n}{2}$ on both sides of the above formula, we have

$$\frac{\left(v^{n+1}+v^n\right)^\intercal \left(v^{n+1}-v^n\right)}{2\tau} = -\frac{\left(v^{n+1}+v^n\right)^\intercal}{2} \cdot \frac{Ru^{n+1}+Ru^n}{2}.$$

Therefore, we obtain that

$$\left(v^{n+1}\right)^{\mathsf{T}}\left(v^{n+1}\right)-(v^n)^{\mathsf{T}}(v^n)=-\left(u^{n+1}\right)^{\mathsf{T}}R\cdot\left(u^{n+1}\right)-(u^n)^{\mathsf{T}}R\cdot(u^n),$$
$$\left(v^{n+1}\right)^{\mathsf{T}}\left(v^{n+1}\right)+\left(u^{n+1}\right)^{\mathsf{T}}\left(R\cdot u^{n+1}\right)=(v^n)^{\mathsf{T}}(v^n)+(u^n)^{\mathsf{T}}(R\cdot u^n),$$

which is $\omega^{n+1}=\omega^n$. Taking into account the symmetric positivity of M^* (28), H_1 (31), and S_2(36), there exists C such that $C^{\mathsf{T}}\cdot C=R$, which yields

$$(u^n,R\cdot u^n)=(C\cdot u^n)^{\mathsf{T}}(C\cdot u^n).$$

Therefore, we obtain

$$w^n=(v^n,v^n)+(C\cdot u^n,C\cdot u^n).$$

□

Theorem 4. *For the nonlinear good Boussinesq Equation (2) with periodic boundary conditions, the schemes CHOC-A, CHOC-B, CHOC-C, and HOC satisfy the following discrete conservation law:*

$$\overline{u^n}=h\sum_{j=1}^{NX}u_j^n\equiv\overline{u^0} \tag{47}$$

provided that $\overline{v^0}=0$.

Proof. Firstly, we consider scheme CHOC-A to solve nonlinear system (2) and have the following formula:

$$u^{n+1}=u^n+\tau\left(\frac{v^n+v^{n+1}}{2}\right),v^{n+1}=v^n+\frac{\tau}{2}N\left(u^{n+1}+u^n\right)+\frac{\tau}{2}H\left[(u^n)^2+\left(u^{n+1}\right)^2\right]. \tag{48}$$

By calculation, we obtain that

$$v^{n+1}=v^n+\frac{\tau}{2}\left(E-\frac{\tau^2}{4}N\right)^{-1}\left\{\tau Nv^n+2Nu^n+H\left[(u^n)^2+\left(u^{n+1}\right)^2\right]\right\}. \tag{49}$$

We construct the following iterative algorithm:

$$\begin{aligned}v_{(k+1)}^{n+1}&=v^n+\frac{\tau}{2}\left(E-\frac{\tau^2}{4}N\right)^{-1}\left\{\tau Nv^n+2Nu^n+H\left[(u^n)^2+\left(u_{(k)}^{n+1}\right)^2\right]\right\},\\ u_{(k+1)}^{n+1}&=u^n+\tau\left(\frac{v^n+v_{(k+1)}^{n+1}}{2}\right),\end{aligned} \tag{50}$$

where $k=0,1,\ldots$ and $u_{(0)}^{n+1}=u^n$. Then, we find that

$$\lim_{k\to\infty}u_{(k)}^{n+1}=u^{n+1},\lim_{k\to\infty}v_{(k)}^{n+1}=v^{n+1}. \tag{51}$$

Considering $\overline{v^0}=0$ and the symmetry of N,H, we can obtain $\overline{v_{(k+1)}^{n+1}}=\overline{v^n}=0,\overline{u_{(k+1)}^{n+1}}=\overline{u^n}$. The limit (51) yields $\overline{v^{n+1}}=0,\overline{u^{n+1}}=\overline{u^n}$. The conservation identity (47) for schemes CHOC-B, CHOC-C, and HOC can be derived similarly.

For the linear good Boussinesq Equation (1), we have the following equivalent Hamiltonian system:

$$\begin{cases}u_t=v,\\ v_t=u_{xx}-u_{xxxx},\end{cases} \tag{52}$$

with the Hamiltonian function $H = -\frac{1}{2}\int \left(v^2 + u_x^2 + u_{xx}^2 + V^2(u)\right)dx$. Thus, we obtain the symplectic conservation law as follows:

$$w(t) = \int du \wedge dvdx = w(0). \tag{53}$$

Symplectic schemes for Hamiltonian systems are proven to be more efficient than non-symplectic schemes for long-time numerical computations and are widely applied to practical problems arising in many fields of science and engineering. These include celestial mechanics, quantum physics, statistics, and so on (see [16,29–31]). Next, we will demonstrate that the considered schemes are symplectic. □

Theorem 5. *For linear GB Equation (1), the schemes CHOC-A, CHOC-B, CHOC-C, and HOC are symplectic with the following conservation law:*

$$w^n = h\sum_{j=1}^{NX} du_j^n \wedge dv_j^n = w^0. \tag{54}$$

Proof. For (38), scheme $CHOC - A$ has the formula as follows:

$$\begin{bmatrix} -\frac{\tau}{2}N & E \\ E & -\frac{\tau}{2}E \end{bmatrix}\begin{bmatrix} U^{n+1} \\ V^{n+1} \end{bmatrix} = \begin{bmatrix} \frac{\tau}{2}N & E \\ E & \frac{\tau}{2}E \end{bmatrix}\begin{bmatrix} U^{n} \\ V^{n} \end{bmatrix}.$$

Therefore, through extensive calculation, scheme CHOC-A is shown to be symplectic. Similarly, the schemes CHOC-B, CHOC-C, and HOC are also symplectic. □

5. Numerical Experiments

In this section, we present some numerical results to illustrate the above theoretical analysis of the CHOC and HOC schemes, mainly focusing on the convergence and discrete conservation laws for numerical solutions of the GB equation. Our numerical results were obtained via MATLAB 2022a.

First, for the linear GB equation, we take the initial value $f(x) = sin(x)$ and exact solution $u(x,t) = \sin(x)\cos\left(\sqrt{2}t\right)$. Here, we focus on issues within a limited space–time domain $[0, 2\pi] \times [0, T]$. The L_2 and L_∞ norms of the errors between the numerical solution and exact solution are defined, respectively, as

$$\|e^n(h,\tau)\|_2 = \sqrt{h\sum_j \left(U_j^n - u_j^n\right)^2}, \quad \|e^n(h,\tau)\|_\infty = \max_j \left|U_j^n - u_j^n\right|,$$

where $U_j^n = u\left(x_j, t_n\right)$ is the exact solution and u_j^n is the numerical solution. The convergence order in the space and time directions is defined as $order1$ and $order2$, respectively,

$$order1 = \frac{\ln(\|e(h_1,\tau)\|/\|e(h_2,\tau)\|)}{\ln(h_1/h_2)}, \quad order2 = \frac{\ln(\|e(h,\tau_1)\|/\|e(h,\tau_2)\|)}{\ln(\tau_1/\tau_2)}.$$

First, we test the convergence order of $CHOC - A$, $CHOC - B$, $CHOC - C$, HOC and take different step sizes in the direction to be considered, while taking a very small step size in the other direction.

Table 6 lists the errors of the numerical solution and exact solution under the L_2 and L_∞ norms, as well as the spatial convergence order calculated with $order1$ for the four schemes while taking different spatial step sizes. In order to render the error in the time direction relatively negligible, we take the time step size $\tau = 10^{-4}$.

Next, Table 7 shows the ratio of the numerical errors in Table 6, calculated with

$$\frac{\text{Numerical error by } CHOC-B \text{ or } CHOC-C}{\text{Numerical error by } CHOA \text{ scheme}}.$$

Table 8 shows the ratio of the numerical errors in Table 6 calculated with

$$\frac{\text{Numerical error by } CHOC-B \text{ or } CHOC-C}{\text{Numerical error by } HOC \text{ scheme}}.$$

Table 9 lists the errors of the numerical solution and exact solution under the L_2 and L_∞ norms, as well as the time convergence order calculated with *order*2 when the four schemes take different time step sizes. In order to render the error in the spatial direction relatively negligible, we take the spatial step size $h = \frac{2\pi}{80}$.

This indicates that the two additional CHOC schemes derived from CHOC-A are more accurate than the CHOC-A and HOC schemes.

Secondly, for the linear principal part of the GB equation, we simulate the discrete conservation law (46) in time interval $[0, 15]$, which is measured with the following approximate motion-invariant error: $\omega^n - \omega^0$.

Thirdly, we consider the nonlinear GB equation (2) with an exact solitary wave solution as follows:

$$u(x,t) = -A\,\mathrm{sech}^2\left[\left(\frac{P}{2}\right)(\xi - \xi_0)\right], \quad \xi = x - ct, \quad (x,t) \in [-50,50] \times [0,1],$$

where $0 < P < 1$, $A = \frac{3P^2}{2}$, $\xi_0 = \left(1 - P^2\right)^{1/2}$. Below, we take a moderate amplitude $A = 0.5$, $\xi_0 = 0$ and take step sizes $h = 0.5$, $\tau = 0.01$. We simulate the discrete conservation law (47) in time interval $[0, 15]$, which is measured with the following approximate motion-invariant error: $\overline{u^n} - \overline{u^0}$. We also test three CHOC schemes for the interaction of two solitary waves governed by the nonlinear GB equation. In this work, we set different amplitudes A of 1 and 0.25, with corresponding initial phases ξ of -60 and -80, respectively. We also take step sizes $h = 0.5$, $\tau = 0.01$. The experimental results indicate that all three *CHOC* schemes effectively simulate the interaction of the two solitary waves, and the results are similar. Therefore, we only present the simulation results for the CHOC-C scheme at different time instances.

Table 6. Numerical errors of u_j^n with $\tau = 10^{-4}$.

h	*Scheme*	$\|e^n\|_2$	**Order**	$\|e^n\|_\infty$	**Order**
$\frac{2\pi}{5}$	$CHOC-A$	7.629×10^{-3}	–	4.1841×10^{-3}	–
	$CHOC-B$	7.4229×10^{-4}	–	3.9829×10^{-4}	–
	$CHOC-C$	9.4958×10^{-4}	–	5.0952×10^{-4}	–
	HOC	8.7936×10^{-4}	–	6.1928×10^{-4}	–
$\frac{2\pi}{10}$	$CHOC-A$	4.203×10^{-4}	4.1816	2.3058×10^{-4}	4.1816
	$CHOC-B$	9.4353×10^{-6}	6.2978	5.0628×10^{-6}	6.2977
	$CHOC-C$	1.348×10^{-5}	6.1384	7.2331×10^{-6}	6.1384
	HOC	2.4481×10^{-5}	5.1667	1.3136×10^{-5}	5.5590
$\frac{2\pi}{15}$	$CHOC-A$	8.0998×10^{-5}	4.0609	4.5682×10^{-5}	3.9927
	$CHOC-B$	7.9367×10^{-7}	6.1054	4.4533×10^{-7}	5.9952
	$CHOC-C$	1.1673×10^{-6}	6.0338	6.5498×10^{-7}	5.9236
	HOC	2.1169×10^{-6}	6.0374	1.1878×10^{-6}	5.9272

Table 6. *Cont.*

h	*Scheme*	$\|e^n\|_2$	Order	$\|e^n\|_\infty$	Order
$\frac{2\pi}{20}$	$CHOC-A$	2.5403×10^{-5}	4.0307	1.4288×10^{-5}	4.0402
	$CHOC-B$	1.3599×10^{-7}	6.1321	7.6726×10^{-8}	6.1129
	$CHOC-C$	2.0994×10^{-7}	5.9636	1.1844×10^{-7}	5.9448
	HOC	3.7792×10^{-7}	5.9893	2.1322×10^{-7}	5.9702
$\frac{2\pi}{25}$	$CHOC-A$	1.0361×10^{-5}	4.0190	5.8447×10^{-6}	4.0059
	$CHOC-B$	3.2376×10^{-8}	6.4316	1.823×10^{-8}	6.4406
	$CHOC-C$	5.7932×10^{-8}	5.7701	3.262×10^{-8}	5.7784
	HOC	1.0185×10^{-7}	5.8760	5.7347×10^{-8}	5.8850

Table 7. The ratio of the numerical errors among different CHOC schemes of u_j^n with $\tau = 10^{-4}$.

h	$CHOC-B$		$CHOC-C$	
	Rate e_2^u	*Rate* e_∞^u	*Rate* e_2^u	*Rate* e_∞^u
$\frac{2\pi}{5}$	0.097	0.095	0.124	0.122
$\frac{2\pi}{10}$	0.022	0.022	0.032	0.031
$\frac{2\pi}{15}$	0.0098	0.0097	0.0144	0.0143
$\frac{2\pi}{20}$	0.0053	0.0054	0.0083	0.0083
$\frac{2\pi}{25}$	0.0031	0.0031	0.0056	0.0056

Table 8. The ratio of the numerical errors among different schemes of u_j^n with $\tau = 10^{-4}$.

h	$CHOC-B$		$CHOC-C$	
	Rate e_2^u	*Rate* e_∞^u	*Rate* e_2^u	*Rate* e_∞^u
$\frac{2\pi}{5}$	0.8441	0.6432	1.8	0.8228
$\frac{2\pi}{10}$	0.3854	0.3854	0.5506	0.5506
$\frac{2\pi}{15}$	0.3749	0.3749	0.5514	0.5514
$\frac{2\pi}{20}$	0.3598	0.3598	0.5555	0.5555
$\frac{2\pi}{25}$	0.3179	0.3179	0.5688	0.5688

Table 9. Verification of temporal convergence rate with $h = \frac{2\pi}{80}$.

τ	*Scheme*	$\|e^n\|_2$	Order	$\|e^n\|_\infty$	Order
$\frac{1}{40}$	$CHOC-A$	5.5718×10^{-6}	–	1.1056×10^{-5}	–
	$CHOC-B$	5.574×10^{-6}	–	1.106×10^{-5}	–
	$CHOC-C$	5.574×10^{-6}	–	1.106×10^{-5}	–
	HOC	5.574×10^{-6}	–	1.106×10^{-5}	–
$\frac{1}{80}$	$CHOC-A$	1.4094×10^{-6}	1.9831	2.8058×10^{-6}	1.9783
	$CHOC-B$	1.4116×10^{-6}	1.9814	2.8101×10^{-6}	1.9764
	$CHOC-C$	1.4116×10^{-6}	1.9814	2.8101×10^{-6}	1.9764
	HOC	1.4116×10^{-6}	1.9814	2.8101×10^{-6}	1.9764
$\frac{1}{160}$	$CHOC-A$	3.5297×10^{-7}	1.9975	7.0373×10^{-7}	1.9953
	$CHOC-B$	3.5515×10^{-7}	1.9908	7.0808×10^{-7}	1.9886
	$CHOC-C$	3.5514×10^{-7}	1.9909	7.0806×10^{-7}	1.9887
	HOC	3.5514×10^{-7}	1.9909	7.0807×10^{-7}	1.9887

Table 9. *Cont.*

τ	*Scheme*	$\|e^n\|_2$	Order	$\|e^n\|_\infty$	Order
$\frac{1}{320}$	$CHOC-A$	8.689×10^{-8}	2.0223	1.7336×10^{-7}	2.0213
	$CHOC-B$	8.907×10^{-8}	1.9954	1.7772×10^{-7}	1.9943
	$CHOC-C$	8.9065×10^{-8}	1.9955	1.777×10^{-7}	1.9944
	HOC	8.9069×10^{-8}	1.9954	1.7771×10^{-7}	1.9944
$\frac{1}{640}$	$CHOC-A$	2.0124×10^{-8}	2.1103	4.0162×10^{-8}	2.1099
	$CHOC-B$	2.2307×10^{-8}	1.9974	4.4534×10^{-8}	1.9966
	$CHOC-C$	2.2301×10^{-8}	1.9978	4.4511×10^{-8}	1.9972
	HOC	2.2305×10^{-8}	1.9976	4.452×10^{-8}	1.9970

Finally, we give three-dimensional waveform diagrams of the exact solution and numerical solution of the three schemes. We also give a comparison between the numerical solution and the exact solution.

6. Conclusions

In this work, for a GB equation, we construct three combined high-order compact symplectic schemes, which are $CHOC-A$, $CHOC-B$, and $CHOC-C$. The schemes satisfy the discrete conservation laws corresponding to the structure-preserving property of the GB equation. Equations (46), (47) and (54) indicate the types of stability of the schemes. $CHOC$ schemes improve the efficiency of the traditional HOC method in simulating such differential equations with multiple-order spatial derivatives, such as GB equations. $CHOC$ schemes make full use of the information of all of the involved derivative values, which leads to fewer nodes and higher-accuracy schemes. Therefore, it mitigates the difficulties of boundary treatment. Finally, the $CHOC$ scheme is more accurate than the HOC scheme with the same order.

In the numerical experiments, we first test the convergence order of $CHOC-A$, $CHOC-B$, $CHOC-C$, and HOC by taking different step sizes in the direction to be considered and taking very small step sizes in the other direction. In Table 6, we list the spatial convergence order of $CHOC-A$, $CHOC-B$, $CHOC-C$, and HOC. We can observe that scheme $CHOC-A$ is of fourth-order accuracy in space. Schemes $CHOC-B$, $CHOC-C$, and HOC are of sixth-order accuracy in space. In line with Tables 7 and 8, we can conclude that $CHOC-B$ and $CHOC-C$ are more accurate for the GB equation than $CHOC-A$ and HOC, and $CHOC-B$ is also superior to $CHOC-C$. In Table 9, we list the time convergence order of $CHOC-A$, $CHOC-B$, $CHOC-C$, and HOC. We can observe that the schemes are of two orders in time. Also, from Figure 1, we can observe that the $CHOC-C$ scheme effectively simulate the interaction of the two solitary waves with the nonlinear GB Equation (2).

Second, from the approximate motion-invariant error simulation depicted in Figures 2–5, we can see that the three $CHOC$ schemes and the HOC scheme satisfy the discrete conservation law (46) for linear GB equations.

Next, we observe Figures 6–9. We find that the errors are small enough; in other words, the three $CHOC$ schemes and the HOC scheme satisfy the conservation law (47) for nonlinear GB Equation (2).

Finally, we use the three $CHOC$ schemes to numerically simulate the solitary wave solutions with the nonlinear good Boussinesq Equation (2). From Figures 10–13, we can observe that the numerical solutions fit the waveforms of the exact solutions well.

When the equation contains multiple spatial derivatives or there are higher-order derivatives, it may be difficult to accurately solve the discrete formulas for these spatial derivatives. In this case, we can use some software, such as Maple, or perform a simulation through numerical methods. In the future, we will also construct combined compact difference schemes to solve more general Boussinesq equations and other PDEs.

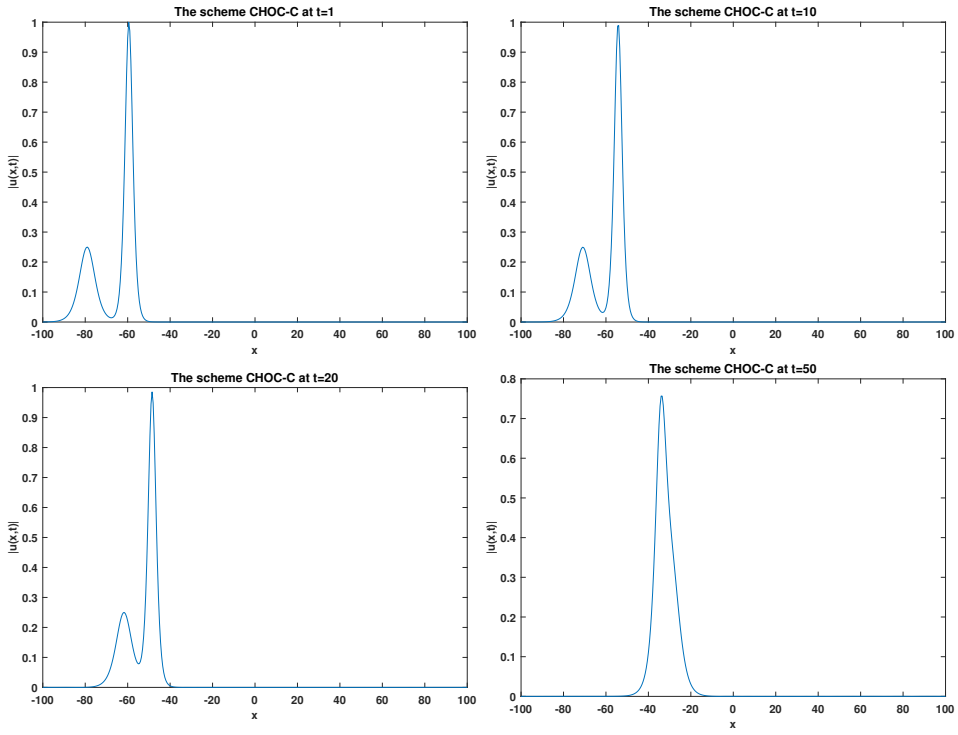


Figure 1. The interaction of two solitary waves in $CHOC-C$, when $h=0.5\,,\tau=0.01$.

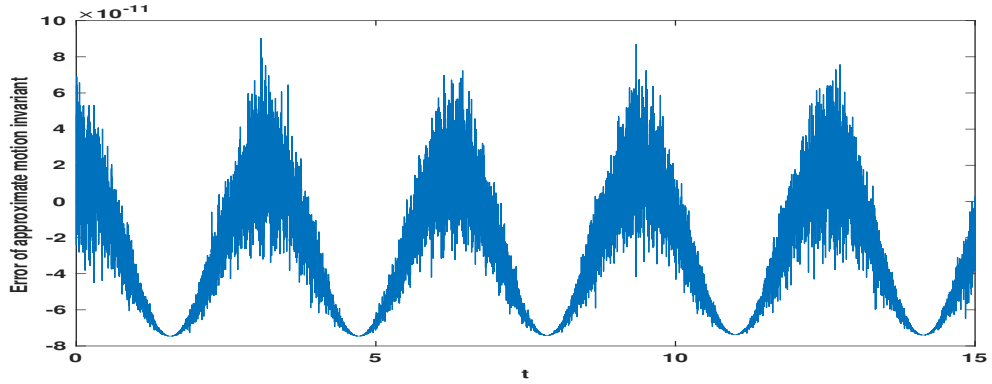


Figure 2. Approximate motion−invariant error diagram for $CHOC-A$ when $h=\frac{2\pi}{80},\tau=0.001$.

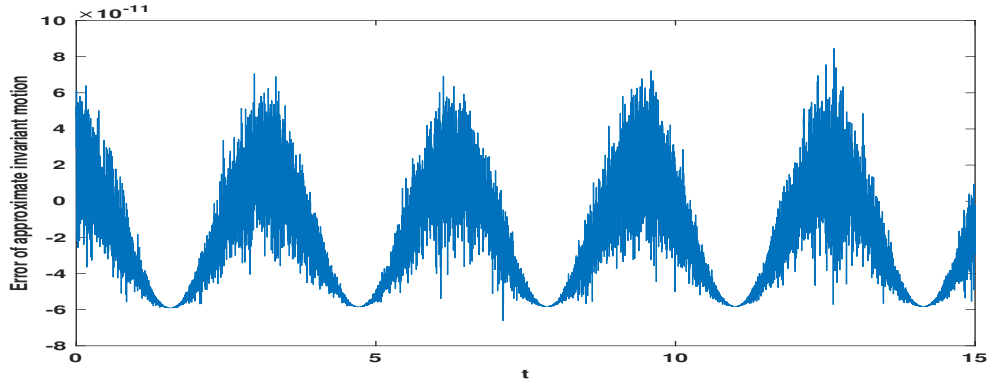


Figure 3. Approximate motion−invariant error diagram for $CHOC-B$ when $h=\frac{2\pi}{80},\tau=0.001$.

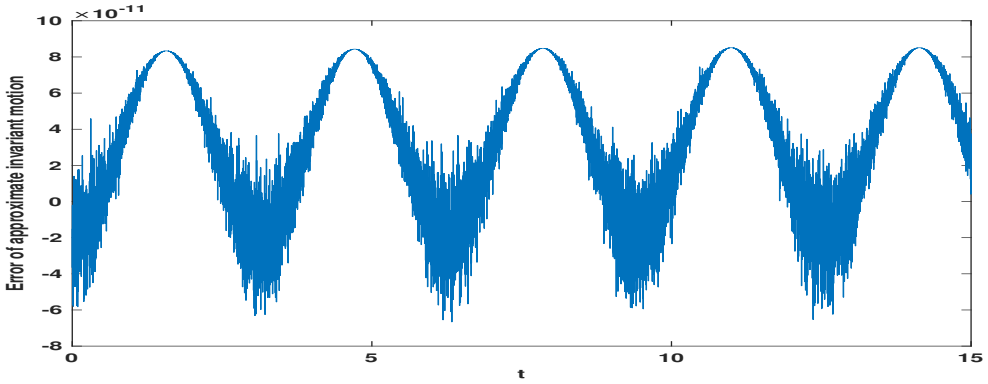


Figure 4. Approximate motion−invariant error diagram for $CHOC-C$ when $h=\frac{2\pi}{80}, \tau=0.001$.

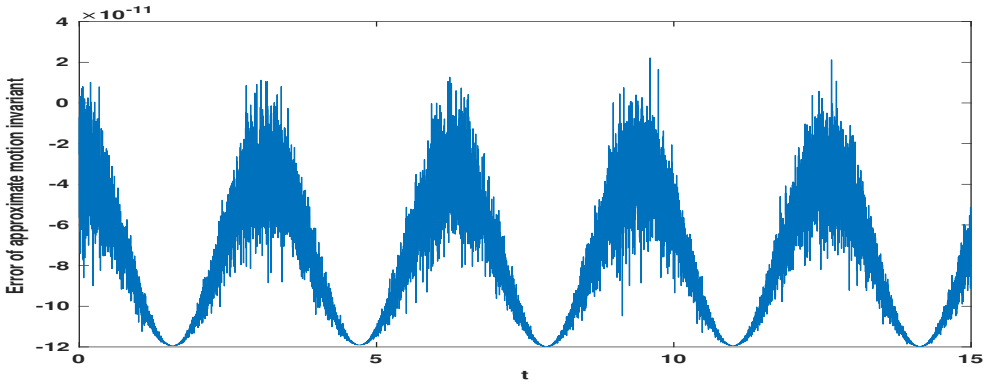


Figure 5. Approximate motion−invariant error diagram for HOC when $h=\frac{2\pi}{80}, \tau=0.001$.

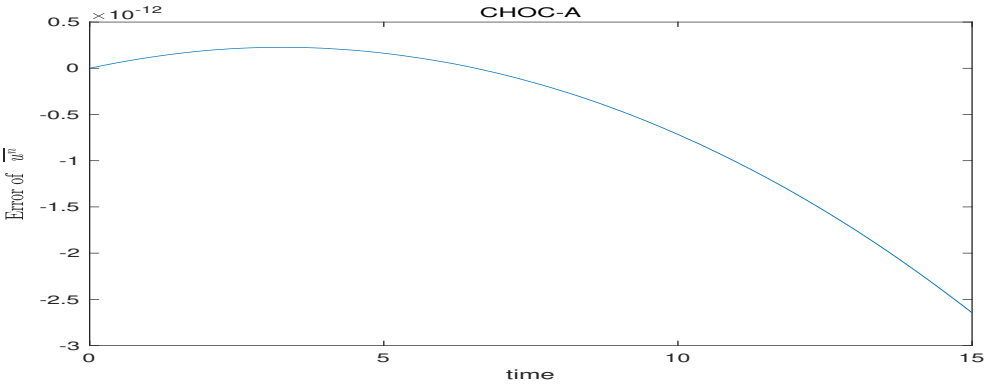


Figure 6. $\overline{u^n}$ error diagram for $CHOC-A$ when $h=0.5, \tau=0.01$.

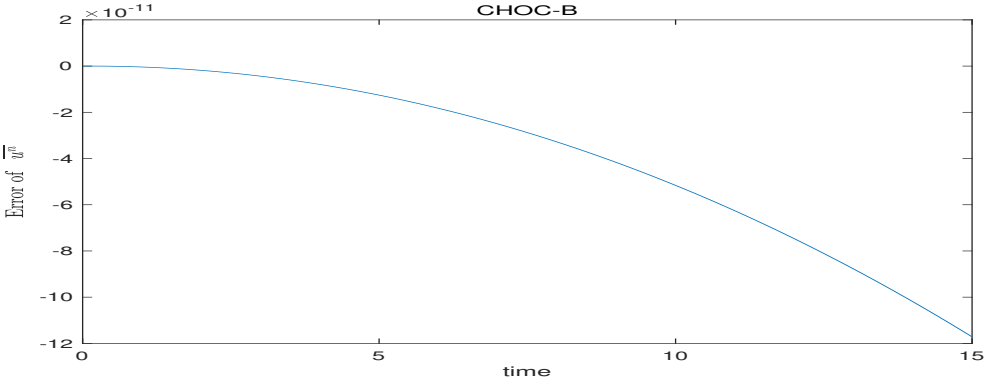


Figure 7. $\overline{u^n}$ error diagram for $CHOC-B$ when $h=0.5, \tau=0.01$.

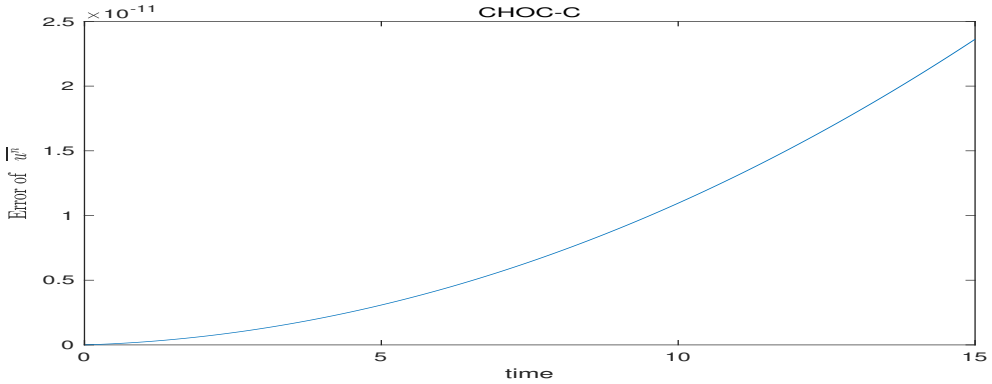


Figure 8. $\overline{u^n}$ error diagram for $CHOC-C$ when $h = 0.5, \tau = 0.01$.

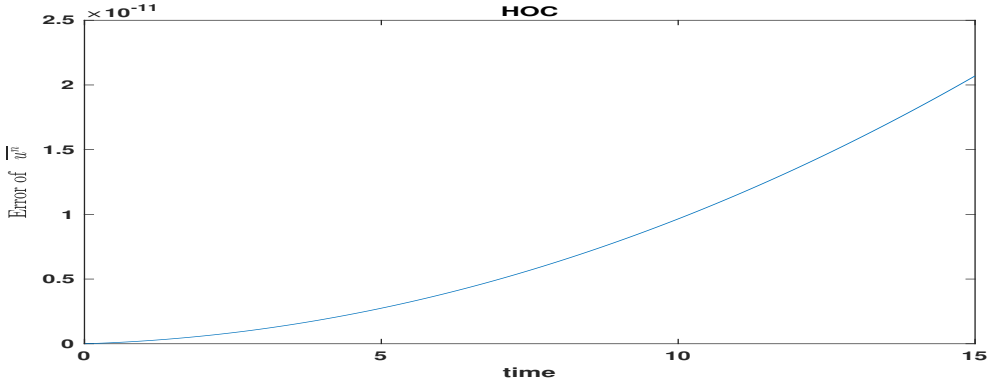


Figure 9. $\overline{u^n}$ error diagram for HOC when $h = 0.5, \tau = 0.01$.

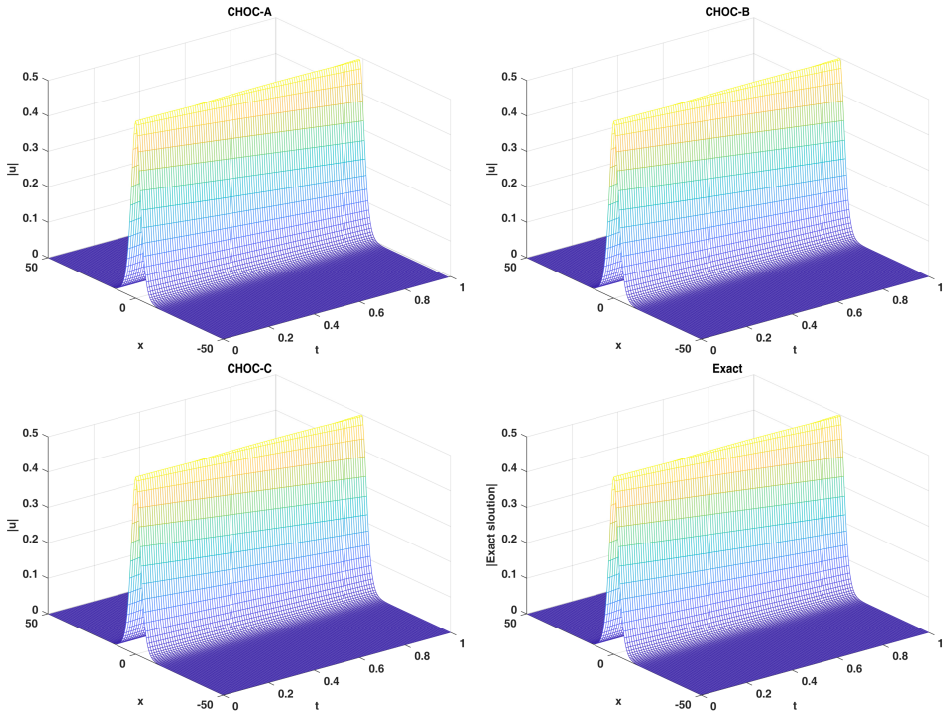


Figure 10. For $h = 0.5, \tau = 0.01$, the three-dimensional waveform diagrams of the $CHOC-A$, $CHOC-B$, and $CHOC-C$ schemes and the three-dimensional waveform diagram of the exact solution are shown.

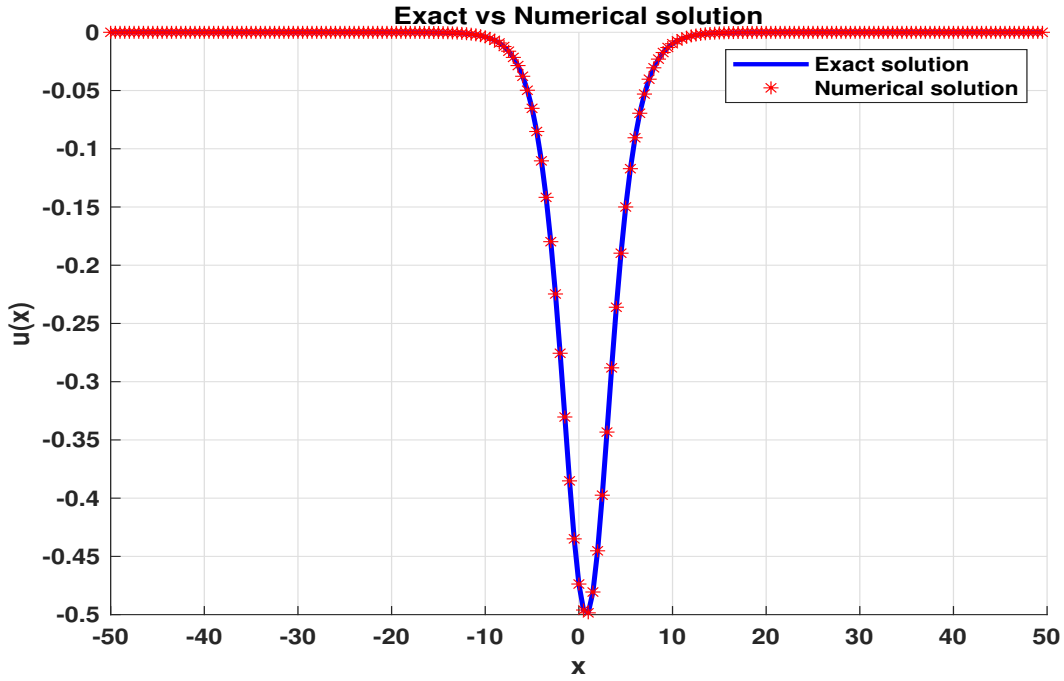


Figure 11. The case of $h = 0.5$, at time $T = 1$. The exact solution vs. the numerical solution of $CHOC - A$.

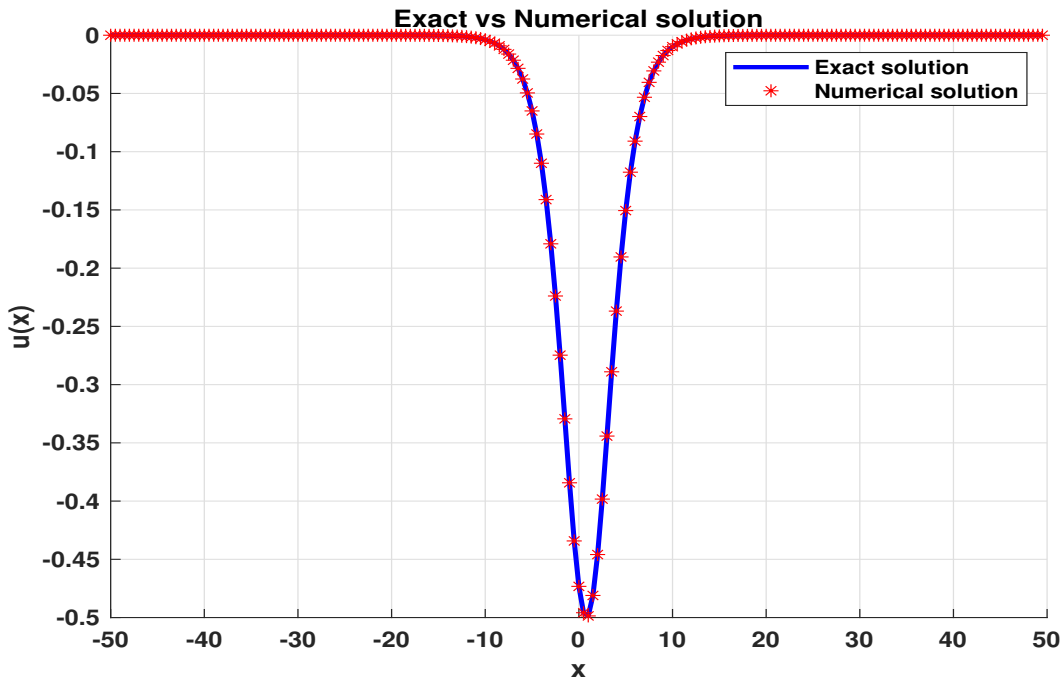


Figure 12. The case of $h = 0.5$, at time $T = 1$. The exact solution vs. the numerical solution of $CHOC - B$.

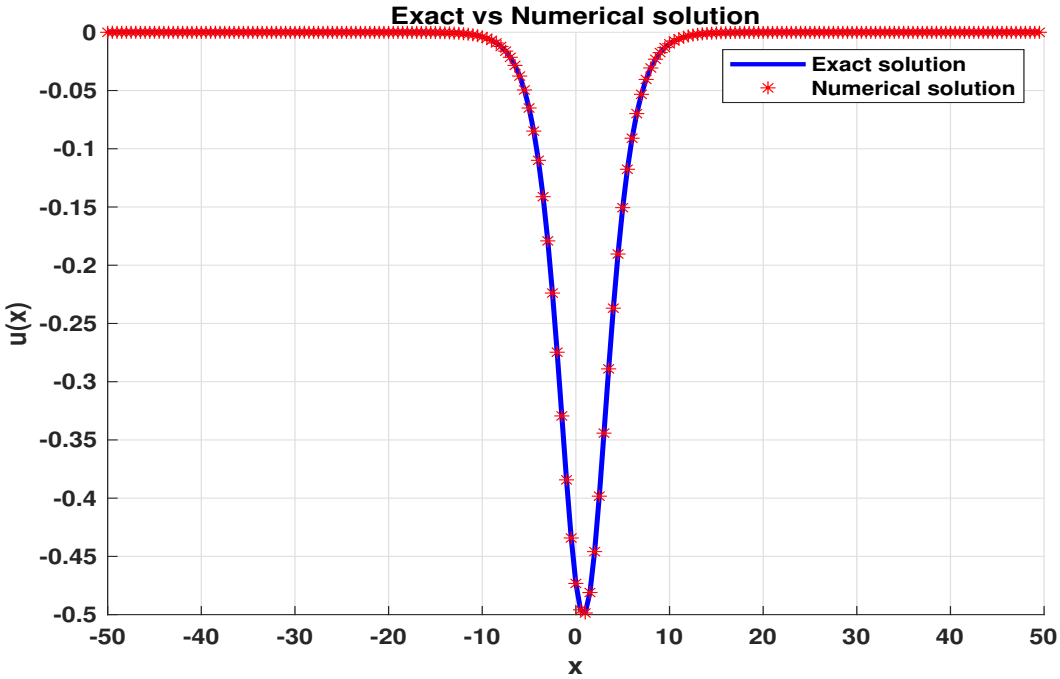


Figure 13. The case of $h = 0.5$, at time $T = 1$. The exact solution vs. the numerical solution of $CHOC - C$.

Author Contributions: Conceptualization, Z.L. and X.Y.; methodology, Z.L. and X.Y.; software, Z.L. and X.Y.; validation, Z.L., X.Y., Y.L., Z.C., and S.K.; formal analysis, Z.L. and X.Y.; investigation, Z.L., X.Y., Y.L., Z.C., and S.K.; resources, X.Y.; data curation, Z.L. and X.Y.; writing—original draft preparation, Z.L. and X.Y.; writing—review and editing, Z.L. and X.Y.; visualization, Z.L. and X.Y.; supervision, X.Y.; project administration, X.Y.; funding acquisition, X.Y. All authors have read and agreed to the published version of the manuscript.

Funding: This work is supported by the Natural Science Foundations of Shandong (No. ZR2023MA062, ZR202204010001), the Science and Technology Plan Project of Dezhou (No. 2021dzkj1638) and the Research Platform Project of Dezhou University (No. 2023XKZX024).

Institutional Review Board Statement: Not applicable.

Informed Consent Statement: Not applicable.

Data Availability Statement: The original contributions presented in the study are included in the article, further inquiries can be directed to the corresponding author. (Matlab 2022a codes can be provided if required).

Conflicts of Interest: The authors declare no conflicts of interest

References

1. Manotanjan, V.S.; Mitchell, A.R.; Morris, J.L. Numerical solutions of the good Boussinesq equation. *Siam. J. Sci. Stat. Comput.* **1984**, *5*, 946–957. [CrossRef]
2. Manotanjan, V.S.; Ortega, T.; Sanz-Serna, J.M. Soliton and antisoliton interactions in the "good" Boussinesq equation. *J. Math. Phys.* **1988**, *29*, 1964–1968. [CrossRef]
3. Ortega, T.; Sanz-Serna, J.M. Nonlinear stability and convergence of finite-difference methods for the "good" Boussinesq equation. *Numer. Math.* **1990**, *58*, 215–229. [CrossRef]
4. Guo, Z.W.; Jiang, T.S.; Vasil'ev, V.I.; Wang, G. Complex structure-preserving method for Schrodinger equations in quaternionic quantum mechanics. *Numer. Algorithms* **2023**, *150*, 1–17. [CrossRef]
5. Iqbal, A.; Abd Hamid, N.N.; Ismail, A.I.M. Soliton Solution of Schrödinger Equation Using Cubic B-Spline Galerkin Method. *Fluids* **2019**, *4*, 108. [CrossRef]
6. Iqbal, A.; Abd Hamid, N.N.; Ismail, A.I.M. Cubic B-spline Galerkin method for numerical solution of the coupled nonlinear Schrödinger equation. *Math. Comput. Sim.* **2020**, *174*, 32–44. [CrossRef]

7. Jiang, T.S.; Wang, G.; Guo, Z.W.; Zhang, D. Algebraic algorithms for a class of Schrodinger equations in split quaternionic mechanics. *Math. Math. Methods. Appl. Sci.* **2024**, *47*, 5349–5354. [CrossRef]
8. Hu, H.Z.; Chen, Y.P.; Zhou, J.W. Two-grid finite element method for time-fractional nonlinear schrodinger equation. *J. Comput. Math.* **2024**, *42*, 1124–1144. [CrossRef]
9. Jiang, T.S.; Guo, Z.W.; Zhang, D.; Vasil'ev, V.I. A fast algorithm for the Schrödinger equation in quaternionic quantum mechanics. *Appl. Math. Lett.* **2024**, *150*, 108975. [CrossRef]
10. Jiang, T.S.; Zhang, Z.Z.; Jiang, Z.W. Algebraic techniques for Schrodinger equations in split quaternionic mechanics. *Comput. Math. Appl.* **2018**, *75*, 2217–2222. [CrossRef]
11. Wang, L.; Kong, L.H.; Chen, M.; Zhu, P.; Guo, H. Structure-Preserving Combined High-Order Compact Schemes for Multiple Order Spatial Derivatives Differential Equations. *J. Sci. Comput.* **2023**, *96*, 8. [CrossRef]
12. Haq, F.; Islam, I.; Tirmizi, I.A. A numerical technique for solution of the MRLW equation using quartic B-splines. *Appl. Math. Model* **2010**, *34*, 4151–4160. [CrossRef]
13. Chu, P.C.; Fan, C. A three-point combined compact difference scheme. *J. Comput. Phys.* **1998**, *140*, 370–399. [CrossRef]
14. Kaur, Deepti.; R.K. Mohanty. Highly accurate compact difference scheme for fourth order parabolic equation with Dirichlet and Neumann boundary conditions. *Appl. Numer. Math.* **2020**, *378*, 125202.
15. Wang, R.F.; Wang, W.H.; Yang, J.H. Containing High Order Compact Scheme Source of Steady Convection-Diffusion Equation. *Sci. Discov.* **2016**, *4*, 156–160. [CrossRef]
16. Chen, B.; He, D.; Pan, K. A linearized high-order combined compact difference scheme for multidimensional coupled Burgers equations. *Numer. Math. Theor. Methods. Appl.* **2018**, *11*, 299–320. [CrossRef]
17. Yu, C.H.; Wang, D.; He, Z.; Pähtz, T. An optimized dispersion–relation-preserving combined compact difference scheme to solve advection equations. *J. Comput. Phys.* **2015**, *300*, 92–115. [CrossRef]
18. Zhang, C.; Wang, H.; Huang, J.F.; Wang, C.; Yue, X.Y. A second order operator splitting numerical scheme for the "good" Boussinesq equation. *Appl. Numer. Math.* **2017**, *119*, 179–193. [CrossRef]
19. Chen, M.; Kong, L.H.; Hong, Y. Efficient structure-preserving schemes for good Boussinesq equation. *Math. Meth. Appl. Sci.* **2018**, *41*, 1743–1752. [CrossRef]
20. Hu, W.P.; Deng, Z.C. Multi-symplectic method for generalized Boussinesq equation. *Appl. Math. Mech.* **2008**, *29*, 927–932. [CrossRef]
21. Cienfuegos, R.; Barthélemy, E.; Bonneton, P. A fourth-order compact finite volume scheme for fully nonlinear and weakly dispersive Boussinesq-type equations. Part II: Boundary conditions and validation. *Int. J. Numer. Methods Fluids.* **2007**, *53*, 1423–1455. [CrossRef]
22. Frutos, J.D.; Ortega, T.; Sanz-Serna, J.M. Pseudospectral method for the "good" Boussinesq equation. *Math. Comput.* **1991**, *57*, 109–122.
23. Oh, S.; Stefanov, A. Improved local well-posedness for the periodic "good" Boussinesq equation. *J. Differ. Equ.* **2013**, *254*, 4047–4065. [CrossRef]
24. Farah, L.; Scialom, M. On the periodic "good" Boussinesq equation. *Proc. Am. Math. Soc.* **2010**, *138*, 953–964. [CrossRef]
25. Zou, Z.L. Higher order Boussinesq equations. *Ocean Eng.* **1999**, *26*, 767–792. [CrossRef]
26. Ucar, Y.; Esen, A.; Karaagac, B. Numerical solutions of Boussinesq equation using Galerkin finite element method. *Wiley* **2020**, *37*, 1612–1630. [CrossRef]
27. Kong, L.H.; Chen, M.; Yin, X. A novel kind of efficient symplectic scheme for Klein-Gordon-Schrödinger equation. *Appl. Numer. Math.* **2019**, *135*, 481–496. [CrossRef]
28. Lele, S.K. Compact finite difference schemes with spectral-like solution. *J. Comput. Phys.* **1992**, *103*, 16–42. [CrossRef]
29. Bridges, T.J.; Reich, S. Multi-symplectic integrators: Numerical schemes for Hamiltonian PDEs that conserve symplecticity. *Phys. Lett. A* **2001**, *284*, 184–193. [CrossRef]
30. Shen, J.; Xu, J.; Yang, J. A new class of efficient and robust energy stable schemes for gradient flows. *SIAM Rev.* **2019**, *61*, 474–506. [CrossRef]
31. Jiménez, S.; Vázquez. L. *Some Remarks on Conservative and Symplectic Schemes*; World Scientific: Singapore, 1991; pp. 151–162.

Disclaimer/Publisher's Note: The statements, opinions and data contained in all publications are solely those of the individual author(s) and contributor(s) and not of MDPI and/or the editor(s). MDPI and/or the editor(s) disclaim responsibility for any injury to people or property resulting from any ideas, methods, instructions or products referred to in the content.